Accepted Manuscript

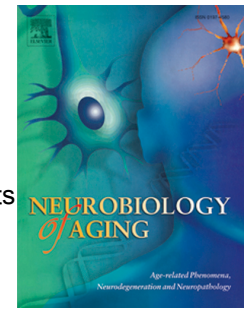

Medium-chain plasma acylcarnitines, ketone levels, cognition, and gray matter volumes in healthy elderly, mildly cognitively impaired or Alzheimer's disease subjects

Domenico Ciavardelli, Fabrizio Piras, Ada Consalvo, Claudia Rossi, Mirco Zucchelli, Carmine Di Ilio, Valerio Frazzini, Carlo Caltagirone, Gianfranco Spalletta, Stefano L. Sensi

PII: S0197-4580(16)00203-7

DOI: 10.1016/j.neurobiolaging.2016.03.005

Reference: NBA 9550

To appear in: *Neurobiology of Aging*

Received Date: 23 June 2015

Revised Date: 2 February 2016

Accepted Date: 6 March 2016

Please cite this article as: Ciavardelli, D., Piras, F., Consalvo, A., Rossi, C., Zucchelli, M., Di Ilio, C., Frazzini, V., Caltagirone, C., Spalletta, G., Sensi, S.L., Medium-chain plasma acylcarnitines, ketone levels, cognition, and gray matter volumes in healthy elderly, mildly cognitively impaired or Alzheimer's disease subjects, *Neurobiology of Aging* (2016), doi: 10.1016/j.neurobiolaging.2016.03.005.

Medium-chain plasma acylcarnitines, ketone levels, cognition, and gray matter volumes in healthy elderly, mildly cognitively impaired or Alzheimer's disease subjects

Domenico Ciavardelli[1, 2]*, Fabrizio Piras[3, 4], Ada Consalvo[5], Claudia Rossi[5], Mirco Zucchelli[5], Carmine Di Ilio[5], Valerio Frazzini[2], Carlo Caltagirone[3, 6], Gianfranco Spalletta[3], Stefano L. Sensi[2, 7]*

[1]School of Human and Social Science, "Kore" University of Enna, Enna, Italy

[2]Molecular Neurology Unit, Center of Excellence on Aging and Translational Medicine (Ce.S.I.-MeT), "G. d'Annunzio" University of Chieti-Pescara, Chieti, Italy

[3]Department of Clinical and Behavioral Neurology, Neuropsychiatry Laboratory, IRCCS Santa Lucia Foundation, Rome, Italy

[4]"Enrico Fermi" Centre for Study and Research, Rome, Italy

[5]Department of Medical, Oral, and Biotechnological Sciences, ''G. d'Annunzio'' University of Chieti-Pescara, Chieti, Italy

[6]Department of Neuroscience, University "Tor Vergata", Rome, Italy

[7]Departments of Neurology and Pharmacology, and Institute for Memory Impairments and Neurological Disorders, University of California-Irvine, Irvine, CA, USA

Running title: Alteration of acylcarnitine metabolism and ketogenesis in AD

*Correspondence to:
DomenicoCiavardelli
School of Human and Social Science,
''Kore'' University of Enna,
Via della Cooperazione, 94100, Enna, Italy.
Tel. +39 0935 536364
Fax +39 0935 536943
e-mail: domenico.ciavardelli@unikore.it;d.ciavardelli@unich.it

Stefano L. Sensi,
Molecular Neurology Unit, (CeSI-MeT),
University "G. d'Annunzio",
Via dei Vestini, 31, Chieti 66100, Italy.
Tel: +39 0871 541544
Fax: +39 0871 541542
e-mail: ssensi@uci.edu

Abstract

Aging, amyloid deposition, and tau-related pathology are key contributors to the onset and progression of Alzheimer's disease (AD). However, AD is also associated with brain hypometabolism and deficits of mitochondrial bioenergetics. Plasma acylcarnitines (ACCs) are indirect indices of altered fatty acid beta-oxidation (FAO) and ketogenesis has been found to be decreased upon aging. Furthermore, in elderly subjects, alterations in plasma levels of specific ACCs have been suggested to predict conversion to Mild Cognitive Impairment (MCI) or AD. In this study, we assayed plasma profiles of ACCs in a cohort of healthy elderly (HC), MCI subjects, and AD patients. Compared to HC or MCI subjects, AD patients showed significant lower plasma levels of several medium-chain ACCs. Furthermore, in AD patients, these lower concentrations were associated with lower prefrontal gray matter volumes and the presence of cognitive impairment. Interestingly, lower levels of medium-chain ACCs were also found to be associated with lower plasma levels of 2-hydroxybutyric acid. Overall, these findings suggest that altered metabolism of medium-chain ACCs and impaired ketogenesis can be metabolic features of AD.

Keywords

Medium-chain acylcarnitines; ketogenesis; targeted metabolomics; fatty acid beta-oxidation; cognitive decline.

1. Introduction

Aging, amyloid deposition, and tau-related pathology are key contributors to the onset and progression of Alzheimer's disease (AD; Herrup, 2010). Impaired energy metabolism has also been associated with brain aging and suggested to favour AD (Costantini et al., 2008; Mosconi et al., 2008). In that respect, compelling evidence indicate that age-dependent metabolic changes promote mitochondrial, endosomal-lysosomal as well as peroxisomal dysfunctions. All these phenomena play a role in the development of AD-related neuronal loss and cognitive decline (Cataldo et al., 2000; Kou et al., 2011; Lin and Beal, 2006; Perez et al., 2015).

Glucose hypometabolism is an important early feature of the AD brain. Furthermore, several studies have indicated a direct correlation by which the occurrence of more severe degrees of hypometabolism can predict a more precipitous course of the disease (Cunnane et al., 2011; de Leon et al., 1983; Dukart et al., 2013; Frackowiak et al., 1981; Jack Jr. et al., 2010; Lehmann et al., 2013). Mechanisms involved in AD-related glucose hypometabolism are not completely known but evidence indicate that defective brain glucose transport, altered glycolysis, or amyloid beta (Aβ)-dependent deregulation of mitochondrial function as well as Aβ–mediated neurotoxicity participate in AD progression and development (Sullivan and Brown, 2005; Winkler et al., 2015). Chronic glucose hypometabolism also acts, indirectly, on the modulation of enzymatic activities that promote oxidative stress, another major contributing factor to AD pathogenesis (Mosconi et al., 2008).

Compelling evidence indicate that mitochondria play a pivotal role in AD-related hypometabolism (Chen and Zhong, 2013; Readnower et al., 2011). In preclinical AD models, mitochondrial deficits have been shown to precede the appearance of plaque deposition and neurofibrillary tangles, thereby supporting the idea that the organelle dysfunction is an early modulator of the AD-related pathological cascade (Yao et al., 2009). In that respect, decreased expression or activity of several mitochondrial enzymes such as pyruvate dehydrogenase, isocitrate dehydrogenase, alpha-ketoglutarate dehydrogenase (αKGDH), and cytochrome C oxidase (COX; Bubber et al., 2005) have been found in the AD brain. Similar findings have been shown in preclinical AD models (Ciavardelli et al., 2010; Rhein et al., 2009). Interestingly, AD-related mitochondrial deficits also occur outside of the Central Nervous System (CNS). In that regard, COX deficiency, decreased activity of αKGDH, and altered mitochondrial fission and fusion have been described to occur in lymphocytes, platelets, and fibroblasts of AD patients (Leuner et

al., 2012; Sorbi et al., 1983; Wang et al., 2008) as well as in skeletal muscles of preclinical AD models (Schuh et al., 2014).

Furthermore, it is conceivable that when standard energetic sources are falling behind, the AD brain is forced to rely on alternative energy substrates. In this view, ketone bodies may play an important role (Iadecola, 2015; VanItallie, 2015). Ketone bodies are produced by the catabolism of fatty acids (FA), a process operated by liver mitochondria. Interestingly, functional deficits in hepatic mitochondrial and/or peroxisomal FA metabolism have been indicated as potential contributors to AD-related cognitive impairment (Astarita and Piomelli, 2011). Moreover, in aging rats, decreased hepatic peroxysomal FA beta-oxidation (FAO) has been linked to the development of alterations in the lipid composition of the brain (Yang et al., 2014).

Alterations of hepatic FAO can affect brain functioning. In that regard, ketone bodies are substrates that, in elderly subjects, may become an energetic source to be used, for brain functioning, as alternative to glucose. This concept is supported by findings indicating that healthy elderly brains increase consumption of energy substrates that are alternative to glucose when glucose utilization decreases, thereby suggesting a compensatory role played by these metabolites in coping with brain energy demand (Hoyer et al., 1991).

Plasma acylcarnitines (ACCs) are indirect indicators of hepatic FAO (Schooneman et al., 2015, 2013; Villarreal-Pérez et al., 2014). Furthermore, free carnitine and ACCs play a significant role in the modulation of brain metabolism (Jones et al., 2010). Of note, specific plasma ACCs have been found to be decreased in healthy elderly subjects converting to MCI or AD (Mapstone et al., 2014).

In this study, we evaluated plasma ACC levels in a cohort of AD patients, MCI subjects, and age-matched healthy controls (HC). Correlations between levels of ACCs, plasma 2-hydroxybutyric acid (b-HBA), and degrees of cognitive competence, assessed with the Mini-Mental State Examination (MMSE), were also evaluated in the three study groups. Finally, structural changes occurring in brains of the three cohorts were investigated with voxel-based morphometry (VBM) and magnetic resonance imaging (MRI). These structural volumes were then correlated with ACC levels.

2. Materials and methods

2.1. Participants and ethics committee

A cohort of 107 individuals of whom 35 were suffering from probable AD, 38 had a diagnosis of MCI, and 34 were healthy matched volunteers was enrolled for this study. AD and MCI patients were recruited by the memory clinic of the Santa Lucia Foundation (Rome, Italy). All individuals recruited as eligible for the study went through clinical examination, neuropsychological testing, and MRI. Subjects gave written informed consent to a research protocol approved by the Joint Ethics Committee of the Santa Lucia Foundation.

HC were recruited through local advertisements and were screened using an extensive neuropsychological test battery in order to exclude subjects with dementia or mild cognitive impairment. To obtain a global index of cognitive impairment, we employed the MMSE (Folstein et al., 1975). MMSE scores were adjusted for age and education level (Measso et al., 1993). The instrument is brief and easy to administer and is widely used to screen for cognitive deterioration (Tsoi et al., 2015). Subjects were also asked to perform the Multiple Features Targets Cancellation Task (MFTC; Gainotti et al., 2001), a test that assesses visuospatial explorative abilities and psychomotor processing speed, the Immediate Visual Memory task (Gainotti et al., 1978), and the face recognition Benton test (Benton et al., 1983). Moreover, we administered the Copy and Delayed Recall of Rey-Osterrieth's complex picture test (CROP and ROPR, respectively; Osterrieth, 1944) and the Freehand Copying of Drawings with and without landmarks (Gainotti et al., 1977) to evaluate visual perception/constructional praxis, perceptual organizational skills, planning, and problem-solving. We also chose several tests from the mental deterioration battery (MDB; Carlesimo et al., 1996) to provide information about functioning of different cognitive domains such as language (MDB Sentence Construction), verbal memory [MDB Rey's 15-word Immediate Recall (RIR) and Delayed Recall (RDR)], logical reasoning [MDB Raven's Progressive Matrices' 47 (PM47)], and language [MDB Phonological (PVF), and Semantic (SVF) Verbal Fluency]. Finally, set-shifting, cognitive flexibility and resistance to interference were assessed using the Modified Wisconsin Card Sorting Test (MWCST; Heaton et al., 1999). None of the HC subjects showed signs of cognitive deficits (Table 1, Supplementary Table 1).

In the MCI group, diagnosis of amnestic multi-domain MCI was made by trained neurologists who interviewed patients and next-of-kin (Petersen and Morris, 2005). Adopted criteria for MCI were: 1) subjective memory impairment confirmed by a score below the normality cut-off in at least one episodic memory test of the MDB or presence of impairment in cognitive

areas other than memory (Supplementary Table 1); 2) lack of fulfillment of National Institute of Health/National Institute on Aging (NIH/NIA)criteria for dementia (McKhann et al., 2011); 3) presence of normal scores on Instrumental Activities of Daily Living (IADL) and a total Clinician Dementia Rating scale (CDR) score of 0.5, consistently with minimal impairment in daily living activities; 4) lack of any evidence and clinical signs of neurological and psychiatric disorders that could be responsible for memory deficits; 5) MRI scans lacking signs of focal lesions as computed according to the semi-automated method recently published by our group (Iorio et al., 2013; minimal diffuse changes or minimal lacunar lesions of white matter were however allowed); 6) absence of signs of moderate-to-severe depression and/or anxiety as confirmed by scores on Beck's Depression Inventory and Hamilton Anxiety Rating scale (14 was the cut-off score for both scales).

AD patients met clinical criteria established by the NIH/NIA and the Alzheimer's Association (McKhann et al., 2011). According to these criteria, we selected AD patients with mild disease severity and a CDR score of 1.0. All the AD subjects were sampled at the time of the diagnosis and none was taking acetylcholinesterase inhibitors or psychotropic drugs (antidepressants, benzodiazepines, and antipsychotics). Normative data and cut-off scores on neuropsychological tests calibrated for the Italian population were employed (Carlesimo et al., 1996). Exclusion criteria were: 1) major medical illnesses; 2) comorbidity with primary psychiatric or neurological disorders (e.g., schizophrenia, major depression, stroke, Parkinson's disease, seizure disorders, head injuries with loss of consciousness); 3) substance abuse or addiction according with the DSM-IV and IV-TR criteria; 4) lack of a reliable caregiver, defined as someone enforcing patient compliance with assessment procedures as well as able to keep in touch with the patient at least twice a week (with at least one personal visit per week); 5) MRI evidence of parenchymal abnormalities or neoplasms. White matter lesions were considered present if radiological finding of hyperintense regions were found on proton-density (PD)/T2–weighted images. Evidence of a single prior ischemic or hemorrhagic event, multiple lacunar infarcts or microhemorrhages (2 or more), cerebral contusions, encephalomalacia, aneurysms, vascular malformations, subdural hematoma, or space-occupying lesions (e.g., arachnoid cysts or brain tumors, such as meningioma) were also set as exclusion criteria; and 6) Hachinski score higher than 4. Finally, patients with cognitive deficits secondary to systemic disorders like unbalanced diabetes, heart diseases, or other major medical illnesses, were excluded.

The demographic and clinical features of the study subjects are summarized in Table 1.

HC, MCI, and AD patients did not significantly differ for age, gender, and diabetes prevalence. HC subjects showed higher education levels compared to AD patients. In all the study participants, using the Abbott Architect system (Abbott, Illinois, USA) in accordance with manufacturer instructions, we assessed plasma levels of glucose, albumin, and triglyceride as well as the enzymatic activity of glutamate-oxaloacetate transaminase (GOT) and glutamic-pyruvate transaminase (GPT). All the analyses revealed no differences among the three cohorts (Table 1).

2.2. Cognitive and behavioural assessments

Two trained neuropsychologists made the cognitive and behavioural assessments while two trained physicians (a neurologist and a psychiatrist) established the diagnosis. Inter-rater reliability levels for the diagnostic procedure and the neuropsychological and illness awareness assessment were set at $k>0.80$. The MMSE was administered to obtain a global index of cognitive functioning. The Neuropsychiatric Inventory (NPI; Cummings et al., 1994) was employed to measure the presence and or severity of neuropsychiatric symptoms. Mean values of MMSE scores and NPI total scores of HC, MCI, and AD subjects are shown in Table 1. NPI total scores were higher in MCI and AD patients compared to HC. Furthermore, AD patients had higher NPI total scores compared to MCI subjects.

2.3. Measurement of plasma acylcarnitine and 2-hydroxybutyric acid (b-HBA) concentrations

Blood samples (10 mL) were, after overnight fasting (11±1 hours), collected from forearm veins in BD Vacutainer TM tubes containing ethylenediaminetetracetic acid (Beckton Dickinson, Franklin Lakes, NJ). Plasma aliquots were prepared by centrifugation at 3000 rpm and 4°C for 15 minutes and stored at -80°C until analysis. Direct Injection Mass Spectrometry (DIMS) analysis of plasma samples was performed, as previously described (Rizza et al., 2014), using the NeoBase non-derivatized MSMS Kit (Perkin Elmer Life and Analytical Sciences, Turku, Finland). Briefly, 100 µL of the extraction solution (NeoBase Non-derivatized Assay Solution, Perkin Elmer) containing internal standards were added to plasma samples (10 µL). Stable isotopes labeled internal standards, target analytes, MS transition and abbreviations are listed in Supplementary Table 2. The liquid chromatography coupled with tandem mass spectrometry (LC-MS/MS) system consisted of a Waters Alliance HT 2795 HPLC Separation Module coupled to a Waters Quattro Ultima Pt ESI

tandem quadrupole mass spectrometer. The instrument was operated in positive electrospray ionization mode using MassLynx V4.0 Software (Waters Corporation, Milford, MA, USA) with auto data processing by NeoLynx (Waters). DIMS analysis was performed injecting 30 µL of sample solutions into the ion source directly by a narrow peek tube. An isocratic run using the flow solvent solution (NeoBase Non-derivatized Assay Solution, Perkin Elmer) as mobile phase was performed. The following changes in flow rate were applied: 0.200 mL min^{-1} for 0.350 min; 0.030 mL min^{-1} for 0.500 min; 0.045 mL min^{-1} for 0.25 min; 0.5 mL min^{-1} for 0.200 min. Total run time was 1.8 minutes. The mass spectrometer ionization source settings were optimized for maximum ion yields for each analyte (Supplementary Table 2). Capillary voltage was 3.5 kV, source temperature was 120°C, desolvation temperature was 350°C, and the collision cell gas pressure was 3-3.50*10^{-3} mbar Argon. All data are expressed as µmol L^{-1}.

Plasma levels of b-HBA were measured by an enzymatic spectophotometric EnzyChrom™ ketone body assay kit (EKBD-100; BioAssay Systems, Hayeard, CA, USA) according to manufacturer instructions. 5µL of plasma were used for the measurement. Absorbance at 340 nm was measured in a Spectra max 190 microplate reader (Molecular Devices, Sunnyvale, CA, USA). b-HBA concentrations were further confirmed by gas-chromatography coupled to mass spectrometry (GC-MS; Bomba et al., 2013). Plasma samples (100 µL) were treated with cold 0.1% (V/V) methanolictrichloroacetic acid (200 µL) and internal standard ($^{13}C_4$ succinic acid; IS) was added to give a final concentration of 10 µg mL^{-1}. Samples were centrifuged at 17000 g for 30 min and 100 µL supernatants were collected and dried in a SpeedVac™ system (Thermo Scientific, Milan, Italy). Dried extracts were derivatized with 20 µL of 20 mg mL^{-1} of methoxyamine hydrochloride (Sigma-Aldrich, Shnelldorf, Germany) solution in pyridine for 60 min at 70°C followed by reaction with 20 µL of N,O-bis(trimethylsilyl)trifluoroacetamide with 1% of trimethylchlorosilane (Sigma-Aldrich) for 60 min at 70°C. GC-MS analysis was performed using a 6890N gas-chromatograph equipped with a 7863 Series auto-sampler and coupled with a 5973N mass spectrometer (Agilent Technologies, Palo Alto, CA, USA) that operated in electron impact ionization mode. Three microliters were injected in pulsed-splitless mode by applying a pressure of 80 psi. The injector temperature was kept at 250°C. Chromatographic separations were performed using a fused silica capillary column HP-5MS (30m x 0.25 mm, Agilent Technologies). Helium was used as carrier gas at a constant flow rate of 1 mL min^{-1}. The GC oven was programmed as follows: start at 70°C (hold time 1 min) raised at 4°C min^{-1} to 300°C (hold time 5 min). The mass spectrometer was automatically calibrated using per-fluorotributylamine as

calibration standard. For quantification, the mass spectrometer was used in the selective ion monitoring mode and mass spectra were recorded in positive modes by monitoring the following ions: m/z 191 for b-HBA and 251 for $^{13}C_4$ succinic acid (IS). Mass spectrometer parameters were: interface temperature: 300°C, ion source: 250°C, and quadrupole: 150°C. Quantification of b-HBA was performed using the external standard method and the IS correction (Bomba et al., 2013). To further validate the analysis, we also employed the standard addition method. To that aim, we used unspiked samples and two 400 and 800ng mL^{-1} b-HBA spikes (n=3). The standard addition analysis provided values that were in agreement with those obtained with the external standard method. Data acquisition was performed using the G1701CA ChemStation software (Agilent Technologies).

2.4. Image acquisition and data processing

All the study subjects underwent the same imaging protocol which included standard clinical sequences (FLAIR, DP-T2-weighted) and a whole-brain 3D high-resolution T1-weighted sequence acquired with a 3T Allegra MR imager (Siemens, Erlangen, Germany). Volumetric whole-brain T1-weighted images were obtained in the sagittal plane using a modified driven equilibrium Fourier transform (MDEFT) sequence (TE/TR = 2.4/7.92 ms, flip angle 15º, voxel-size 1x1x1 mm3). All planar sequence acquisitions were obtained in the plane of the AC–PC line. Particular care was taken to center subjects head in the head coil and to restrain their movements with cushions. T1-weighted images were processed and examined by using the SPM8 software (Wellcome Department of Imaging Neuroscience Group, London, UK; http://www.fil.ion.ucl.ac.uk/spm) and the VBM8 toolbox (http://dbm.neuro.uni-jena.de/vbm.html) running in Matlab 2007b (MathWorks, Natick, MA, USA). The toolbox extends the unified segmentation model (Ashburner and Friston, 2005) consisting of MRI field intensity inhomogeneity correction, spatial normalization and tissue segmentation at several pre-processing steps to further improve the quality of data pre-processing. At the beginning, to increase the signal-to-noise ratio in the data, an optimized block wise nonlocal-means filter (Coupé et al., 2006) was applied to MRI scans using the Rician noise adaption (Wiest-Daessle et al., 2008). After that step, an adaptive maximum “ex post” segmentation approach extended by partial volume estimation was employed to divide MRI scans into gray matter (GM), white matter (WM) and Cerebro-Spinal Fluid (CSF). The segmentation step was finished by applying a spatial constraint to the segmented tissue probability maps based on a

hidden Markow Random Field model (Cuadra et al., 2005). The process was performed to remove isolated voxels that were unlikely to be part of a certain tissue class and to close holes in clusters of connected voxels of a certain class, thereby producing a higher signal-to-noise ratio of the final tissue probability maps. Finally, the iterative high-dimensional normalization approach, provided by the Diffeomorphic Anatomical Registration Through Exponentiated Lie Algebra (DARTEL; Ashburner, 2007; Bergouignan et al., 2009) toolbox, was applied to the segmented tissue maps in order to register them to the stereotactic space of the Montreal Neurological Institute (MNI). Tissue deformations were used to modulate participants GM tissue maps and compare volumetric differences across groups. Voxel values of the resulting normalized and modulated GM segments indicated the probability (between 0 and 1) that a specific voxel belonged to the relative tissue. Finally, modulated and normalized GM segments were written with an isotropic voxel resolution of 1.5 mm^3 and smoothed with an 8 mm FWHM Gaussian kernel. Segmented, normalized, modulated and smoothed GM images were then used for analyses.

2.5. Statistical analysis

One-way analysis of the variance (ANOVA) followed by Fischer LSD post-hoc test was performed in order to highlight main differences between each study group. When the assumption of the homogeneity of the variance was rejected by Levene test, the Kruskal-Wallis test followed by multiple comparisons of mean ranks was performed. Correlations between plasma analyte concentrations and neuropsychological scores were assessed by Spearman's correlation analysis. Unsupervised hierarchical cluster analysis and supervised multivariate partial least squares-discriminant analysis (PLS-DA) was performed after data mean centering, unit variance scaling (van den Berg et al., 2006), and log transformation of metabolite concentrations. Variable Importance in Projection (VIP) scores were calculated by estimating the importance of each variable used in the PLS-DA model. A variable with a VIP score higher than one is considered important in the PLS-DA model (Le Cao et al., 2008). Receiver operating characteristic (ROC) analysis was performed using the ROC curve analysis tool ROCCET (ROC curve explorer and tester available at http://www.roccet.ca) (Xia et al., 2013). Correction for multiple comparisons was performed using the false discovery rate (FDR) method. Corrected p-values were considered statistically significant when less than 0.050. Statistical analysis was performed using Statistica 6.0 (Statsoft, Tulsa, OK) software and MetaboAnalyst statistical analysis module (Xia et al., 2009).

Volumetric GM differences were assessed by ANOVA and single group-by-group t-tests. To identify the brain regions in which patients showed GM volumetric changes that correlated with ACC levels, several multiple regression models (separating group – i.e. HC, MCI and AD, and biological measures – i.e. ACCs) were adopted using the biological measure as regressor and age as covariate of no interest. Statistical analyses were carried out at voxel level using SPM8 (www.fil.ion.ucl.ac.uk/spm/software/spm8). Correlations were considered statistically significant when $p<0.050$ as assessed with Family-Wise Error (FWE) correction, a procedure accounting for multiple testing. Correlation analysis took in account only spatially-contiguous clusters with a size of 30 voxels or greater. Finally, to obtain fine anatomical localization of statistical results, the Automated Anatomical Labeling (AAL; Tzourio-Mazoyer et al., 2002) was used. The procedure allows the inclusion of all the main gyri and sulci of the cerebral cortex and subcortical and deep GM structures for a total of 90 anatomical volumes of interest.

3. Results

3.1. Plasma ACC profiles of the study cohort

Plasmatic ACC concentrations were measured in HC, MCI, and AD subjects (Fig. 1 and Supplementary Table 3). Plasma levels of several medium-chain ACCs such as octanoylcarnitine (C8), decenoylcarnitine (C10:1), decanoylcarnitine (C10), dodecenoylcarnitine (C12:1), lauroylcarnitine (C12), tetradecenoylcarnitine (C14:1), and tetradecadienoylcarnitine (C14:2) and other ACCs such as oleylcarnitine (C18:1) and acetyl carnitine (C2) were found to be lower in AD patients compared to HC or MCI subjects. Furthermore, compared to MCI subjects, free carnitine (C0) levels were significantly lower in AD patients. No differences in plasma levels of other short-chain, dicarboxy or β-hydroxy-ACCs were found. Within-group correlation maps of plasma ACCs were built for HC individuals (Fig. 2A), MCI subjects (Fig. 2B), and AD patients (Fig. 2C). Significant associations between medium-chain ACCs, ranging from C8 to C14:2, were found in each study group.

3.2. Assessment of ACCs as disease biomarkers by multivariate and ROC data analysis

The ACC predictive power to discriminate between HC, MCI, and AD subjects was tested by unsupervised hierarchical clustering and supervised PLS-DA approaches. A heatmap visualization (Fig. 3A), a commonly used feature for unsupervised clustering, as well as a PLS-DA score plot (Fig. 3B) showed that AD patients can be, in part, set apart from MCI and HC subjects. However, both methods failed to segregate HC subjects from MCI individuals. As for PLS-DA, the R^2Y was 0.486, thereby indicating a low discriminating power of the model. We also checked the predictive power of this model by evaluating the Q^2Y. Q^2Y was found to be lower than 0.500 (Q^2Y=0.271), thereby suggesting poor predictive power of the PLS-DA model. Medium-chain ACCs stood as the main discriminating variable accounting for the separation of AD patients from HC and MCI subjects (Fig. 3C). VIP scores were in fact higher than 1 for C8 to C14:2 ACCs.

To assess the sensitivity and specificity of single ACCs or ratios between ACC pairs, we performed ROC analysis. A ROC curve can be described as the area under the curve (AUC), a parameter that indicates the test strength where an ideal marker should give an AUC=1. In contrast, AUC values less than 0.7 indicate poor classification accuracy. Single ACCs were found to be poor predictors and unable to discriminate between the three study groups. Therefore, we evaluated ACC ratios. ACC ratios have been often shown to be better indicators of disease and/or physiological status compared to absolute ACC concentrations (Hall et al., 2014; Krug et al., 2012). Figures 3E and 3F show ROC analyses based on best predictor ratios. Improved prediction power was observed when analysis was performed on ratio of ACC pairs. The C12:1/C14 ratio was found useful for discriminating between HC and AD subjects (AUC=0.800; sensitivity=80%; specificity=60%) while the C14:1/C14 ratio did separate MCI from AD patients (AUC=0.818; sensitivity=70%; specificity=80%). We did not find single ACC values or ratios between ACC pairs that could, with acceptable specificity and selectivity, differentiate between MCI and HC subjects (Fig. 3D).

3.3. Correlations between plasmatic ACCs and behavioural performances of the study groups

To assess potential relationships between plasma levels of target metabolites and cognitive performances of study subjects, we investigated, with Spearman correlation analysis, correlations between ACC levels and MMSE or NPI total scores. No significant correlations were found in HC and MCI subjects. In contrast, in AD patients, positive significant correlations appeared when plotting MMSE scores and levels of medium-chain ACCs (Table 2, Supplementary Fig. 1). Finally,

no significant correlations between ACC levels and NPI total scores were found in the AD study group.

3.4. Correlations between plasma ACC profiles and regional gray matter (GM) variations

C10 directly correlates with the other medium-chain ACCs found to be significantly different in the AD group when compared to the HC or MCI. We therefore selected this metabolite as representative for the whole class of medium-chain ACCs. Associations between C10 levels and GM volume changes, assessed by VBM-MRI, were then evaluated in brain areas of HC, MCI, and AD patients. Positive relationships between C10 levels and GM volumes were found in the left or right interface between Brodmann areas (BA) 3-4 and 6 of MCI and AD patients, respectively (Fig. 4, Table 3). The same correlations were confirmed for other medium-chain ACCs such as C8 (Supplementary Fig.2, Supplementary Table 5) and C12 (Supplementary Fig.3, Supplementary Table 6). No significant correlations were found in the HC group.

3.5. Analysis of plasma 2-hydroxybutyric acid (b-HBA) in the study cohort

Plasma concentrations of b-HBA were evaluated in a representative subset of HC, MCI, and AD subjects (n=20; Fig. 5). Analysis was first performed using a standard spectrophotometric assay. b-HBA levels were measurable in HC samples but found to be below the limit of the assay sensitivity in several MCI and AD samples. We therefore decided to assess plasma samples with a GC-MS method that we have previously employed (Bomba et al., 2013).

Mean plasma b-HBA concentrations (and SD) were 24±14, 21±17, and 12±7 $\mu mol\ L^{-1}$ for HC, MCI, and AD, respectively. One-way ANOVA indicated significant differences between the study groups [$F(2, 56)=4.01$, $p=0.022$]. Post-hoc test showed that b-HBA concentrations were significantly lower in AD patients compared to HC ($p=0.008$) and MCI subjects ($p=0.041$; Fig. 5).

Of note, plasma levels of b-HBA positively correlated with levels of C2 and medium-chain ACCs such as C10, C12, C12:1, C14, C14:2, and C14:1 in AD patients (Fig. 6C, Supplementary Table 4). No significant correlations were found between b-HBA levels and levels of short, dicarboxy-ACCs, β-hydroxy-ACCs or long chain ACCs (data not shown). Furthermore, we did not find significant correlations between plasma levels of medium-chain ACCs and b-HBA in HC subjects or MCI patients (Fig. 6A, B). In AD patients, higher b-HBA levels were associated with higher MMSE

scores (ρ=0.51, p=0.026; Fig. 6F). The same correlation was not found in HC or MCI subjects (Fig. 6D, E). Finally, no correlation between b-HBA levels and NPI total scores was found in our study cohorts (data not shown).

4. Discussion

In the present study, we found that, compared to HC or MCI subjects, plasma levels of medium-chain ACCs were significantly lower in AD patients. Plasma levels of medium-chain ACCs have been recently reported to decrease upon physiological aging (Houtkooper et al., 2011) in mice, but, to our knowledge, this is the first report indicating that the phenomenon is also occurring in AD patients. Recently, ACCs such as propionylcarnitine (C3) and 3-hydroxy-hexadecenoylcarnitine (C16:1-OH) have been shown to be predictive of conversion to MCI or AD (Mapstone et al., 2014). In our cohorts, plasma concentrations of C16:1-OH were below the sensitivity of the analytical assay. Furthermore, we did not find significant differences for plasma levels of C3 in the three study groups. However, partially in agreement with the Mapstone study, we found C3 levels in MCI patients (0.4±0.2μmol L^{-1}) that showed a trend toward statistical significance (p=0.083) compared to levels of HC subjects (0.5±0.2μmol L^{-1}). In the same study (Mapstone et al., 2014), the authors did not find significant differences in terms of medium-chain ACCs. However, it should be noted that the study pooled together MCI and AD patients, thereby potentially obliterating the AD-driven effects with the higher medium-chain ACC levels carried by MCI individuals.

The variations in plasma ACC levels that we have found in the AD group are unlikely dependent on the nutritional status of the study subjects. All the study participants showed overlapping plasma levels of glucose, albumin, and triglyceride as well as GOT and GPT activities. NPI appetite/eating sub-scores were also comparable (data not shown), thereby indicating a homogeneous nutritional status across all the study groups.

Using PLS-DA and ROC analysis, we found that ACC ratios singled out AD patients from MCI and HC subjects. In contrast, multivariate and univariate approaches failed to reveal differences between HC and MCI individuals and indicated low predictive power for these metabolites as biomarkers for the two groups. Therefore, medium-chain ACCs do not appear as useful biomarkers to predict phenotypic conversion from HC to MCI.

It is important to emphasize that, in AD patients, levels of medium-chain ACCs correlate with degrees of cognitive performances as assessed by the MMSE. This finding suggests that low levels of medium-chain ACCs may be associated with metabolic changes involved in AD-related cognitive decline. In order to assess whether differential ACC profiles correlate with differences in GM volumes occurring in the brain of MCI and AD patients, we performed a VBM-MRI analysis of scans of the three study groups. The analysis revealed direct correlations between plasma levels of medium-chain ACCs such as C8, C10, and C12 and regional changes in GM volumes that occurred in the precentral gyrus (BA6) of MCI and AD patients. Interestingly, previous studies showed glucose hypometabolism and concurrent BA6 alterations in brains of MCI or AD patients (Barbeau et al., 2008; Canu et al., 2011; Rabinovici et al., 2007; Zheng et al., 2014). The premotor cortex has been shown to be consistently activated in functional MRI studies focused on investigating changes in working memory processes (Owen et al., 2005). This region is in fact known to play a critical role in maintaining memory-related visuospatial attention. Furthermore, a previous VBM-MRI study showed the occurrence of premotor cortical atrophy in MCI patients, thereby offering a neuroanatomical basis for the working memory deficits observed in these patients (Yao et al., 2012). Overall, with the limitation of a cross-sectional study, our findings suggest a structural relationship between brain integrity and plasma levels of medium-chain ACCs, thereby providing preliminary experimental evidence for a working hypothesis postulating that lower plasma concentrations of these metabolites are associated with the progression of AD- or MCI-related regional brain atrophy. The hypothesis needs to be confirmed by future longitudinal studies.

An additional aspect of the study is offered by the fact that ACC plasma levels reflect the metabolite hepatic turnover. The liver accounts for most of the FAO, the process that controls ACC production. Thus, plasma levels of ACCs mainly depend on hepatic ACC metabolism (Schooneman et al., 2015), a phenomenon that has been demonstrated in primates (Bell et al., 1982).

Interestingly, we found that plasma medium-chain ACCs are, in each study group, cross-connected. This finding suggests that lower levels of different medium-chain ACCs that we find in the AD cohort are likely associated with pathological alterations of a common (still undefined) pathway that affects hepatic mitochondrial and/or peroxisomal FAO.

Defective hepatic FAO can eventually lead to impaired ketogenesis and lower levels of plasma ketones (Fukao et al., 2004). This possibility is further supported by the decrease of circulating

free carnitine (C0) found in AD patients as C0 availability is a limiting factor for FAO and regulates hepatic ketogenesis (McGarry et al., 1975). Ketones, like acetoacetate and b-HBA, are energy substrates employed by the brain as alternative to glucose. Ketone bodies counteract neuronal hyperexcitability, another contributing factor to AD-related neuronal loss (Vossel et al., 2013). Therefore, one can speculate that altered peripheral FAO leads to impaired ketogenesis and exacerbates the energy default as well as seizure susceptibility that occurs in the AD brain (Hertz et al., 2015). Regional impairment of glucose uptake and utilization does not affect the brain consumption of ketone bodies, thereby suggesting that, in the AD brain, these molecules act as compensatory energy substrates (Castellano et al., 2015). In that pathological setting, it is conceivable that impairment of hepatic ketogenesis may further exacerbate the brain energetic deficits and be a critical aggravating factor for AD progression.

In order to evaluate the correlation between plasma levels of ACCs and ketogenesis, we assessed plasma b-HBA levels in the three cohorts. Significant lower values were found in AD patients when compared to HC or MCI subjects. It should be emphasized that, in AD patients, plasma b-HBA levels directly correlated with levels of medium-chain ACCs and MMSE scores. The positive correlation, in AD patients, between plasma levels of b-HBA and cognitive performances is not completely surprising. Ketogenic diets and/or pharmacological manipulations aimed at promoting ketogenesis have been shown to improve cognitive performances in preclinical AD models as well as in cognitively impaired subjects or AD patients (Henderson et al., 2009; Reger et al., 2004; Van der Auwera et al., 2005; Yao et al., 2011).

Overall, our findings lay the ground for the hypothesis that alterations of medium-chain ACC metabolism are associated with impaired ketogenesis and can help to exacerbate AD pathology.

5. Conclusions

We have identified several alterations in ACC plasma levels, a biochemical signature that, if confirmed in larger and longitudinal cohorts, can help the diagnostic differentiation of AD patients from age-matched MCI or HC individuals. In our AD cohort, we have found significant lower levels of medium-chain ACCs. This phenomenon can be related to defective functioning of hepatic FAO and, in turn, promote impaired ketogenesis as well as cognitive deficits. Of note, lower plasma

levels of medium-chain ACCs were also found to correlate with regional decrease of GM volumes in MCI and AD brains as well as, in AD patients, with decreased MMSE scores.

The association between levels of medium-chain ACCs and b-HBA may indicate that, in AD patients, deficits of peripheral ACC production go along with impairment of liver ketogenesis and lower availability of ketone bodies. As brain glucose hypometabolism is one AD feature, reduced ketogenesis may play a synergistic detrimental role in exacerbating the energetic default that occurs in the AD brain.

Acknowledgements

SLS is supported by funds from the Italian Department of Education (PRIN, 2008 and 2011) (PRIN2010#2010M2JARJ_005) and funds from the Italian Department of Health (RF-2013-02358785). The authors are in debt to Alberto Granzotto for his help with editing and critical reading.

References

Ashburner, J., 2007. A fast diffeomorphic image registration algorithm. Neuroimage 38, 95–113. doi:10.1016/j.neuroimage.2007.07.007

Ashburner, J., Friston, K.J., 2005. Unified segmentation. Neuroimage 26, 839–851. doi:10.1016/j.neuroimage.2005.02.018

Astarita, G., Piomelli, D., 2011. Towards a whole-body systems [multi-organ] lipidomics in Alzheimer's disease. Prostaglandins. Leukot. Essent. Fatty Acids 85, 197–203. doi:10.1016/j.plefa.2011.04.021

Barbeau, E.J., Ranjeva, J.P., Didic, A., Confort-Gouny, S., Felician, O., Soulier, E., Cozzone, P.J., Ceccaldi, M., Poncet, A., 2008. Profile of memory impairment and gray matter loss in amnestic mild cognitive impairment. Neuropsychologia 46, 1009–1019. doi:DOI 10.1016/j.neuropsychologia.2007.11.019

Bell, F.P., DeLucia, A., Bryant, L.R., Patt, C.S., Greenberg, H.S., 1982. Carnitine metabolism in Macaca arctoides: the effects of dietary change and fasting on serum triglycerides, unesterified carnitine, esterified (acyl) carnitine, and beta-hydroxybutyrate. Am. J. Clin. Nutr. 36, 115–121.

Benton A.L., Sivan A.B., Hamsher K., Varney N.R., S.O., 1983. Facial recognition: stimulus and multiple choice pictures, in: Benton A.L., Sivan A.B., Hamsher K., Varney N.R., S.O. (Ed.), Contributions to Neuropsychological Assessment. New York: Oxford University Pres, pp. 30–40.

Bergouignan, L., Chupin, M., Czechowska, Y., Kinkingnéhun, S., Lemogne, C., Le Bastard, G., Lepage, M., Garnero, L., Colliot, O., Fossati, P., 2009. Can voxel based morphometry, manual segmentation and automated segmentation equally detect hippocampal volume differences in acute depression? Neuroimage 45, 29–37. doi:10.1016/j.neuroimage.2008.11.006

Bomba, M., Ciavardelli, D., Silvestri, E., Canzoniero, L.M.T., Lattanzio, R., Chiappini, P., Piantelli, M., Di Ilio, C., Consoli, A., Sensi, S.L., 2013. Exenatide promotes cognitive enhancement and positive brain metabolic changes in PS1-KI mice but has no effects in 3xTg-AD animals. Cell Death Dis. 4, e612. doi:10.1038/cddis.2013.139

Bubber, P., Haroutunian, V., Fisch, G., Blass, J.P., Gibson, G.E., 2005. Mitochondrial abnormalities in Alzheimer brain: mechanistic implications. Ann. Neurol. 57, 695–703. doi:10.1002/ana.20474

Canu, E., McLaren, D.G., Fitzgerald, M.E., Bendlin, B.B., Zoccatelli, G., Alessandrini, F., Pizzini, F.B.,

Ricciardi, G.K., Beltramello, A., Johnson, S.C., Frisoni, G.B., 2011. Mapping the structural brain changes in Alzheimer's disease: the independent contribution of two imaging modalities. J. Alzheimer's Dis. 26 Suppl 3, 263–274. doi:10.3233/JAD-2011-0040

Carlesimo, G.A., Caltagirone, C., Gainotti, G., 1996. The Mental Deterioration Battery: normative data, diagnostic reliability and qualitative analyses of cognitive impairment. The Group for the Standardization of the Mental Deterioration Battery. Eur. Neurol. 36, 378–384.

Castellano, C.A., Nugent, S., Paquet, N., Tremblay, S., Bocti, C., Lacombe, G., Imbeault, H., Turcotte, E., Fulop, T., Cunnane, S.C., 2015. Lower brain 18F-fluorodeoxyglucose uptake but normal 11C-acetoacetate metabolism in mild Alzheimer's disease dementia. J. Alzheimer's Dis. 43, 1343–1353. doi:10.3233/JAD-141074

Cataldo, A.M., Peterhoff, C.M., Troncoso, J.C., Gomez-Isla, T., Hyman, B.T., Nixon, R.A., 2000. Endocytic pathway abnormalities precede amyloid beta deposition in sporadic Alzheimer's disease and Down syndrome: differential effects of APOE genotype and presenilin mutations. Am. J. Pathol. 157, 277–286.

Chen, Z., Zhong, C., 2013. Decoding Alzheimer's disease from perturbed cerebral glucose metabolism: Implications for diagnostic and therapeutic strategies. Prog. Neurobiol. 108, 21–43. doi:10.1016/j.pneurobio.2013.06.004

Ciavardelli, D., Silvestri, E., Del Viscovo, A., Bomba, M., De Gregorio, D., Moreno, M., Di Ilio, C., Goglia, F., Canzoniero, L.M.T., Sensi, S.L., 2010. Alterations of brain and cerebellar proteomes linked to Aβ and tau pathology in a female triple-transgenic murine model of Alzheimer's disease. Cell Death Dis. 1.

Costantini, L.C., Barr, L.J., Vogel, J.L., Henderson, S.T., 2008. Hypometabolism as a therapeutic target in Alzheimer's disease. BMC Neurosci. 9 Suppl 2, S16. doi:10.1186/1471-2202-9-S2-S16

Coupé, P., Yger, P., Barillot, C., 2006. Fast non local means denoising for 3D MR images. Med. Image Comput. Comput. Assist. Interv. 9, 33–40.

Cuadra, M.B., Cammoun, L., Butz, T., Cuisenaire, O., Thiran, J.-P., 2005. Comparison and validation of tissue modelization and statistical classification methods in T1-weighted MR brain images. IEEE Trans. Med. Imaging 24, 1548–65. doi:10.1109/TMI.2005.857652

Cummings, J.L., Mega, M., Gray, K., Rosenberg-Thompson, S., Carusi, D.A., Gornbein, J., 1994. The Neuropsychiatric Inventory: comprehensive assessment of psychopathology in dementia. Neurology 44, 2308–2314.

Cunnane, S., Nugent, S., Roy, M., Courchesne-Loyer, A., Croteau, E., Tremblay, S., Castellano, A.,

Pifferi, F., Bocti, C., Paquet, N., Begdouri, H., Bentourkia, M., Turcotte, E., Allard, M., Barberger-Gateau, P., Fulop, T., Rapoport, S.I., 2011. Brain fuel metabolism, aging, and Alzheimer's disease. Nutrition 27, 3–20. doi:10.1016/j.nut.2010.07.021

de Leon, M.J., Ferris, S.H., George, A.E., Christman, D.R., Fowler, J.S., Gentes, C., Reisberg, B., Gee, B., Emmerich, M., Yonekura, Y., Brodie, J., Kricheff II, Wolf, A.P., 1983. Positron emission tomographic studies of aging and Alzheimer disease. AJNR Am. J. Neuroradiol. 4, 568–571.

Dukart, J., Kherif, F., Mueller, K., Adaszewski, S., Schroeter, M.L., Frackowiak, R.S.J., Draganski, B., 2013. Generative FDG-PET and MRI model of aging and disease progression in Alzheimer's disease. PLoS Comput. Biol. 9, e1002987. doi:10.1371/journal.pcbi.1002987

Folstein, M.F., Folstein, S.E., McHugh, P.R., 1975. "Mini-mental state". A practical method for grading the cognitive state of patients for the clinician. J. Psychiatr. Res. 12, 189–198.

Frackowiak, R.S., Pozzilli, C., Legg, N.J., Du Boulay, G.H., Marshall, J., Lenzi, G.L., Jones, T., 1981. Regional cerebral oxygen supply and utilization in dementia. A clinical and physiological study with oxygen-15 and positron tomography. Brain 104, 753–778.

Fukao, T., Lopaschuk, G.D., Mitchell, G.A., 2004. Pathways and control of ketone body metabolism: on the fringe of lipid biochemistry. Prostaglandins. Leukot. Essent. Fatty Acids 70, 243–51. doi:10.1016/j.plefa.2003.11.001

Gainotti, G., Caltagirone, C., Miceli, G., 1978. Immediate visual-spatial memory in hemisphere-damaged patients: impairment of verbal coding and of perceptual processing. Neuropsychologia 16, 501–7.

Gainotti, G., Marra, C., Villa, G., 2001. A double dissociation between accuracy and time of execution on attentional tasks in Alzheimer's disease and multi-infarct dementia. Brain 124, 731–8.

Gainotti, G., Miceli, G., Caltagirone, C., 1977. Constructional apraxia in left brain-damaged patients: a planning disorder? Cortex. 13, 109–18.

Hall, P.L., Marquardt, G., McHugh, D.M.S., Currier, R.J., Tang, H., Stoway, S.D., Rinaldo, P., 2014. Postanalytical tools improve performance of newborn screening by tandem mass spectrometry. Genet. Med. 16, 889–95. doi:10.1038/gim.2014.62

Heaton, R.K., Avitable, N., Grant, I., Matthews, C.G., 1999. Further crossvalidation of regression-based neuropsychological norms with an update for the Boston Naming Test. J. Clin. Exp. Neuropsychol. 21, 572–82. doi:10.1076/jcen.21.4.572.882

Henderson, S.T., Vogel, J.L., Barr, L.J., Garvin, F., Jones, J.J., Costantini, L.C., 2009. Study of the

ketogenic agent AC-1202 in mild to moderate Alzheimer's disease: a randomized, double-blind, placebo-controlled, multicenter trial. Nutr Metab 6, 31. doi:10.1186/1743-7075-6-31

Herrup, K., 2010. Reimagining Alzheimer's disease--an age-based hypothesis. J. Neurosci. 30, 16755–16762. doi:10.1523/JNEUROSCI.4521-10.2010

Hertz, L., Chen, Y., Waagepetersen, H.S., 2015. Effects of ketone bodies in Alzheimer's disease in relation to neural hypometabolism, beta-amyloid toxicity, and astrocyte function. J. Neurochem. 134, 7–20. doi:10.1111/jnc.13107

Houtkooper, R.H., Argmann, C., Houten, S.M., Canto, C., Jeninga, E.H., Andreux, P.A., Thomas, C., Doenlen, R., Schoonjans, K., Auwerx, J., 2011. The metabolic footprint of aging in mice. Sci. Rep. 1. doi:Artn 134Doi 10.1038/Srep00134

Hoyer, S., Nitsch, R., Oesterreich, K., 1991. Predominant abnormality in cerebral glucose utilization in late-onset dementia of the Alzheimer type: a cross-sectional comparison against advanced late-onset and incipient early-onset cases. J. Neural Transm. Park. Dis. Dement. Sect. 3, 1–14.

Iadecola, C., 2015. Sugar and Alzheimer's disease: a bittersweet truth. Nat. Neurosci. 18, 477–478. doi:10.1038/nn.3986

Iorio, M., Spalletta, G., Chiapponi, C., Luccichenti, G., Cacciari, C., Orfei, M.D., Caltagirone, C., Piras, F., 2013. White matter hyperintensities segmentation: a new semi-automated method. Front. Aging Neurosci. 5, 76. doi:10.3389/fnagi.2013.00076

Jack Jr., C.R., Knopman, D.S., Jagust, W.J., Shaw, L.M., Aisen, P.S., Weiner, M.W., Petersen, R.C., Trojanowski, J.Q., 2010. Hypothetical model of dynamic biomarkers of the Alzheimer's pathological cascade. Lancet Neurol. 9, 119–128. doi:10.1016/S1474-4422(09)70299-6

Jones, L.L., McDonald, D.A., Borum, P.R., 2010. Acylcarnitines: role in brain. Prog. Lipid Res. 49, 61–75. doi:10.1016/j.plipres.2009.08.004

Kou, J., Kovacs, G.G., Hoftberger, R., Kulik, W., Brodde, A., Forss-Petter, S., Honigschnabl, S., Gleiss, A., Brugger, B., Wanders, R., Just, W., Budka, H., Jungwirth, S., Fischer, P., Berger, J., 2011. Peroxisomal alterations in Alzheimer's disease. Acta Neuropathol. 122, 271–283. doi:10.1007/s00401-011-0836-9

Krug, S., Kastenmüller, G., Stückler, F., Rist, M.J., Skurk, T., Sailer, M., Raffler, J., Römisch-Margl, W., Adamski, J., Prehn, C., Frank, T., Engel, K.-H., Hofmann, T., Luy, B., Zimmermann, R., Moritz, F., Schmitt-Kopplin, P., Krumsiek, J., Kremer, W., Huber, F., Oeh, U., Theis, F.J., Szymczak, W., Hauner, H., Suhre, K., Daniel, H., 2012. The dynamic range of the human metabolome revealed by challenges. FASEB J. 26, 2607–19. doi:10.1096/fj.11-198093

Le Cao, K.A., Rossouw, D., Robert-Granie, C., Besse, P., 2008. A sparse PLS for variable selection when integrating omics data. Stat. Appl. Genet. Mol. Biol. 7, Article 35. doi:10.2202/1544-6115.1390

Lehmann, M., Ghosh, P.M., Madison, C., Laforce Jr., R., Corbetta-Rastelli, C., Weiner, M.W., Greicius, M.D., Seeley, W.W., Gorno-Tempini, M.L., Rosen, H.J., Miller, B.L., Jagust, W.J., Rabinovici, G.D., 2013. Diverging patterns of amyloid deposition and hypometabolism in clinical variants of probable Alzheimer's disease. Brain 136, 844–858. doi:10.1093/brain/aws327

Leuner, K., Schulz, K., Schutt, T., Pantel, J., Prvulovic, D., Rhein, V., Savaskan, E., Czech, C., Eckert, A., Muller, W.E., 2012. Peripheral mitochondrial dysfunction in Alzheimer's disease: focus on lymphocytes. Mol. Neurobiol. 46, 194–204. doi:10.1007/s12035-012-8300-y

Lin, M.T., Beal, M.F., 2006. Mitochondrial dysfunction and oxidative stress in neurodegenerative diseases. Nature 443, 787–795. doi:10.1038/nature05292

Mapstone, M., Cheema, A.K., Fiandaca, M.S., Zhong, X., Mhyre, T.R., MacArthur, L.H., Hall, W.J., Fisher, S.G., Peterson, D.R., Haley, J.M., Nazar, M.D., Rich, S.A., Berlau, D.J., Peltz, C.B., Tan, M.T., Kawas, C.H., Federoff, H.J., 2014. Plasma phospholipids identify antecedent memory impairment in older adults. Nat. Med. 20, 415–418. doi:10.1038/nm.3466

McGarry, J.D., Robles-Valdes, C., Foster, D.W., 1975. Role of carnitine in hepatic ketogenesis. Proc. Natl. Acad. Sci. U. S. A. 72, 4385–4388.

McKhann, G.M., Knopman, D.S., Chertkow, H., Hyman, B.T., Jack Jr., C.R., Kawas, C.H., Klunk, W.E., Koroshetz, W.J., Manly, J.J., Mayeux, R., Mohs, R.C., Morris, J.C., Rossor, M.N., Scheltens, P., Carrillo, M.C., Thies, B., Weintraub, S., Phelps, C.H., 2011. The diagnosis of dementia due to Alzheimer's disease: recommendations from the National Institute on Aging-Alzheimer's Association workgroups on diagnostic guidelines for Alzheimer's disease. Alzheimers Dement 7, 263–269. doi:10.1016/j.jalz.2011.03.005

Measso, G., Cavarzeran, F., Zappala, G., Lebowitz, B.D., Crook, T.H., Pirozzolo, F.J., Amaducci, L.A., Massari, D., Grigoletto, F., 1993. The Mini-Mental-State-Examination - Normative Study of an Italian Random Sample. Dev. Neuropsychol. 9, 77–85.

Mosconi, L., Pupi, A., De Leon, M.J., 2008. Brain glucose hypometabolism and oxidative stress in preclinical Alzheimer's disease. Ann. N. Y. Acad. Sci. 1147, 180–195. doi:10.1196/annals.1427.007

Osterrieth, P.A., 1944. Le test de copie d'une figure complexe. Arch. Psychol. 30, 206–256.

Owen, A.M., McMillan, K.M., Laird, A.R., Bullmore, E., 2005. N-back working memory paradigm: a meta-analysis of normative functional neuroimaging studies. Hum. Brain Mapp. 25, 46–59. doi:10.1002/hbm.20131

Perez, S.E., He, B., Nadeem, M., Wuu, J., Ginsberg, S.D., Ikonomovic, M.D., Mufson, E.J., 2015. Hippocampal endosomal, lysosomal, and autophagic dysregulation in mild cognitive impairment: correlation with abeta and tau pathology. J. Neuropathol. Exp. Neurol. 74, 345–358. doi:10.1097/NEN.0000000000000179

Petersen, R.C., Morris, J.C., 2005. Mild cognitive impairment as a clinical entity and treatment target. Arch. Neurol. 62, 1160–3; discussion 1167. doi:10.1001/archneur.62.7.1160

Rabinovici, G.D., Seeley, W.W., Kim, E.J., Gorno-Tempini, M.L., Rascovsky, K., Pagliaro, T.A., Allison, S.C., Halabi, C., Kramer, J.H., Johnson, J.K., Weiner, M.W., Forman, M.S., Trojanowski, J.Q., Dearmond, S.J., Miller, B.L., Rosen, H.J., 2007. Distinct MRI atrophy patterns in autopsy-proven Alzheimer's disease and frontotemporal lobar degeneration. Am. J. Alzheimers. Dis. Other Demen. 22, 474–488. doi:10.1177/1533317507308779

Readnower, R.D., Sauerbeck, A.D., Sullivan, P.G., 2011. Mitochondria, Amyloid β, and Alzheimer's Disease. Int. J. Alzheimers. Dis. 2011, 104545. doi:10.4061/2011/104545

Reger, M.A., Henderson, S.T., Hale, C., Cholerton, B., Baker, L.D., Watson, G.S., Hyde, K., Chapman, D., Craft, S., 2004. Effects of beta-hydroxybutyrate on cognition in memory-impaired adults. Neurobiol. Aging 25, 311–314. doi:10.1016/S0197-4580(03)00087-3

Rhein, V., Song, X., Wiesner, A., Ittner, L.M., Baysang, G., Meier, F., Ozmen, L., Bluethmann, H., Drose, S., Brandt, U., Savaskan, E., Czech, C., Gotz, J., Eckert, A., 2009. Amyloid-beta and tau synergistically impair the oxidative phosphorylation system in triple transgenic Alzheimer's disease mice. Proc. Natl. Acad. Sci. U. S. A. 106, 20057–20062. doi:10.1073/pnas.0905529106

Rizza, S., Copetti, M., Rossi, C., Cianfarani, M.A., Zucchelli, M., Luzi, A., Pecchioli, C., Porzio, O., Di Cola, G., Urbani, A., Pellegrini, F., Federici, M., 2014. Metabolomics signature improves the prediction of cardiovascular events in elderly subjects. Atherosclerosis 232, 260–264. doi:10.1016/j.atherosclerosis.2013.10.029

Schooneman, M.G., Ten Have, G.A.M., van Vlies, N., Houten, S.M., Deutz, N.E.P., Soeters, M.R., 2015. Transorgan fluxes in a porcine model reveal a central role for liver in acylcarnitine metabolism. Am. J. Physiol. Endocrinol. Metab. 309, E256–64. doi:10.1152/ajpendo.00503.2014

Schooneman, M.G., Vaz, F.M., Houten, S.M., Soeters, M.R., 2013. Acylcarnitines: reflecting or

inflicting insulin resistance? Diabetes 62, 1–8. doi:10.2337/db12-0466

Schuh, R.A., Jackson, K.C., Schlappal, A.E., Spangenburg, E.E., Ward, C.W., Park, J.H., Dugger, N., Shi, G.L., Fishman, P.S., 2014. Mitochondrial oxygen consumption deficits in skeletal muscle isolated from an Alzheimer's disease-relevant murine model. BMC Neurosci. 15, 24. doi:10.1186/1471-2202-15-24

Sorbi, S., Bird, E.D., Blass, J.P., 1983. Decreased pyruvate dehydrogenase complex activity in Huntington and Alzheimer brain. Ann. Neurol. 13, 72–78. doi:10.1002/ana.410130116

Sullivan, P.G., Brown, M.R., 2005. Mitochondrial aging and dysfunction in Alzheimer's disease. Prog. Neuro-Psychopharmacology Biol. Psychiatry 29, 407–410. doi:10.1016/j.pnpbp.2004.12.007

Tsoi, K.K.F., Chan, J.Y.C., Hirai, H.W., Wong, S.Y.S., Kwok, T.C.Y., 2015. Cognitive Tests to Detect Dementia: A Systematic Review and Meta-analysis. JAMA Intern. Med. 175, 1450–8. doi:10.1001/jamainternmed.2015.2152

Tzourio-Mazoyer, N., Landeau, B., Papathanassiou, D., Crivello, F., Etard, O., Delcroix, N., Mazoyer, B., Joliot, M., 2002. Automated anatomical labeling of activations in SPM using a macroscopic anatomical parcellation of the MNI MRI single-subject brain. Neuroimage 15, 273–289. doi:10.1006/nimg.2001.0978

van den Berg, R.A., Hoefsloot, H.C., Westerhuis, J.A., Smilde, A.K., van der Werf, M.J., 2006. Centering, scaling, and transformations: improving the biological information content of metabolomics data. BMC Genomics 7, 142. doi:10.1186/1471-2164-7-142

Van der Auwera, I., Wera, S., Van Leuven, F., Henderson, S.T., 2005. A ketogenic diet reduces amyloid beta 40 and 42 in a mouse model of Alzheimer's disease. Nutr Metab 2, 28. doi:10.1186/1743-7075-2-28

VanItallie, T.B., 2015. Biomarkers, ketone bodies, and the prevention of Alzheimer's disease. Metabolism 64, S51–7. doi:10.1016/j.metabol.2014.10.033

Villarreal-Pérez, J.Z., Villarreal-Martínez, J.Z., Lavalle-González, F.J., Torres-Sepúlveda, M.D.R., Ruiz-Herrera, C., Cerda-Flores, R.M., Castillo-García, E.R., Rodríguez-Sánchez, I.P., Martínez de Villarreal, L.E., 2014. Plasma and urine metabolic profiles are reflective of altered beta-oxidation in non-diabetic obese subjects and patients with type 2 diabetes mellitus. Diabetol. Metab. Syndr. 6, 129. doi:10.1186/1758-5996-6-129

Vossel, K.A., Beagle, A.J., Rabinovici, G.D., Shu, H., Lee, S.E., Naasan, G., Hegde, M., Cornes, S.B., Henry, M.L., Nelson, A.B., Seeley, W.W., Geschwind, M.D., Gorno-Tempini, M.L., Shih, T.,

Kirsch, H.E., Garcia, P.A., Miller, B.L., Mucke, L., 2013. Seizures and epileptiform activity in the early stages of Alzheimer disease. JAMA Neurol 70, 1158–1166. doi:10.1001/jamaneurol.2013.136

Wang, X., Su, B., Fujioka, H., Zhu, X., 2008. Dynamin-like protein 1 reduction underlies mitochondrial morphology and distribution abnormalities in fibroblasts from sporadic Alzheimer's disease patients. Am. J. Pathol. 173, 470–482. doi:10.2353/ajpath.2008.071208

Wiest-Daessle, N., Prima, S., Coupe, P., Morrissey, S.P., Barillot, C., 2008. Rician noise removal by non-Local Means filtering for low signal-to-noise ratio MRI: applications to DT-MRI. Med. Image Comput. Comput. Interv. 11, 171–179.

Winkler, E.A., Nishida, Y., Sagare, A.P., Rege, S. V, Bell, R.D., Perlmutter, D., Sengillo, J.D., Hillman, S., Kong, P., Nelson, A.R., Sullivan, J.S., Zhao, Z., Meiselman, H.J., Wenby, R.B., Soto, J., Abel, E.D., Makshanoff, J., Zuniga, E., De Vivo, D.C., Zlokovic, B. V, 2015. GLUT1 reductions exacerbate Alzheimer's disease vasculo-neuronal dysfunction and degeneration. Nat. Neurosci. 18, 521–530. doi:10.1038/nn.3966

Xia, J., Broadhurst, D.I., Wilson, M., Wishart, D.S., 2013. Translational biomarker discovery in clinical metabolomics: an introductory tutorial. Metabolomics 9, 280–299. doi:10.1007/s11306-012-0482-9

Xia, J., Psychogios, N., Young, N., Wishart, D.S., 2009. MetaboAnalyst: a web server for metabolomic data analysis and interpretation. Nucleic Acids Res. 37, W652–60. doi:10.1093/nar/gkp356

Yang, L., Zhang, Y., Wang, S., Zhang, W., Shi, R., 2014. Decreased liver peroxisomal beta-oxidation accompanied by changes in brain fatty acid composition in aged rats. Neurol. Sci. 35, 289–293. doi:10.1007/s10072-013-1509-3

Yao, J., Chen, S., Mao, Z., Cadenas, E., Brinton, R.D., 2011. 2-Deoxy-D-glucose treatment induces ketogenesis, sustains mitochondrial function, and reduces pathology in female mouse model of Alzheimer's disease. PLoS One 6, e21788. doi:10.1371/journal.pone.0021788

Yao, J., Irwin, R.W., Zhao, L., Nilsen, J., Hamilton, R.T., Brinton, R.D., 2009. Mitochondrial bioenergetic deficit precedes Alzheimer's pathology in female mouse model of Alzheimer's disease. Proc. Natl. Acad. Sci. U. S. A. 106, 14670–14675. doi:10.1073/pnas.0903563106

Yao, Z., Hu, B., Liang, C., Zhao, L., Jackson, M., Alzheimer's Disease Neuroimaging, I., 2012. A longitudinal study of atrophy in amnestic mild cognitive impairment and normal aging revealed by cortical thickness. PLoS One 7, e48973. doi:10.1371/journal.pone.0048973

Zheng, D., Sun, H., Dong, X., Liu, B., Xu, Y., Chen, S., Song, L., Zhang, H., Wang, X., 2014. Executive dysfunction and gray matter atrophy in amnestic mild cognitive impairment. Neurobiol. Aging 35, 548–555. doi:10.1016/j.neurobiolaging.2013.09.007

Table 1. Demographic and clinical features of the study groups. Differences between the study groups were assessed by one factor ANOVA followed by Fischer LSD post-hoc test or Kruskal-Wallis test followed by multiple comparisons of mean ranks and χ^2 test (95% confidence level). p-values less than 0.050 are shown in bold.

Characteristic	HC[a]	MCI[b]	AD[c]	Levene test, p	ANOVA/Kruskal-Wallis test, F[d]/H[e] (p)	HC vs MCI, p[f]	HC vs AD, p[f]	MCI vs AD, p[f]	Observed χ^2; critical χ^2 (p)[g]
Number of participants	34	38	35						
Gender (Male/Female)	17/17	19/19	16/19						0.17; 5.99 (0.92)
Age, mean (SD), years	72 (4)	72 (3)	73 (4)	0.58	0.83(0.44)	0.50	0.56	0.20	
Education level, mean (SD), years	11 (4)	10 (5)	8 (4)	0.084	3.80 **(0.025)**	0.21	**0.007**	0.12	
MMSE[h], mean (SD)	27 (2)	25 (2)	18 (5)	**<0.001**	67.72 **(<0.001)**	**<0.001**	**<0.001**	**<0.001**	
NPI (12 items)[i]	5 (6)	12 (11)	25 (21)	**<0.001**	34.72 **(<0.001)**	**0.008**	**<0.001**	**0.006**	
Diabetes prevalence, n (%)	0 (0)	2 (5)	3 (9)						2.26; 5.99 (0.32)
Glucose, mean (SD), $mgdL^{-1}$	94 (15)	92 (11)	91 (13)	0.47	0.54 (0.58)	0.47	0.31	0.76	
Albumin, mean (SD), $g\ dL^{-1}$	3.9 (0.4)	3.9 (0.3)	3.8 (0.3)	0.49	0.89 (0.41)	0.50	0.18	0.50	
Triglycerides, mean (SD), $mg\ dL^{-1}$	113 (34)	113(57)	110 (40)	0.42	0.03 (0.97)	>0.99	0.83	0.82	
GOT[j], mean (SD), $IU\ L^{-1}$[l]	41 (12)	40 (9)	39 (9)	**0.035**	0.23 (0.89)	>0.99	>0.99	>0.99	
GPT[k], mean (SD), $IU\ L^{-1}$[l]	17 (6)	17 (6)	19 (9)	0.51	0.65 (0.53)	0.86	0.29	0.38	

[a] Healthy controls; [b] Patients with mild cognitive impairment; [c] Patients with Alzheimer's disease; [d] degrees of freedom: 2, 104; [e] degrees of freedom: 2, 107; [f] Fisher LSD post-hoc test or multiple comparisons of mean ranks; [g] degrees of freedom: 2; [h] Mini mental state examination corrected for age and education level; [i] Neuropsychiatric inventory; [j] Glutamate-oxalacetate transaminase; [k] Glutamic-pyruvate transaminase; [l] IU: international units.

Table 2. Significant correlations between acylcarnitine plasma levels and cognitive performances in AD patients. Data are shown as Spearman's correlation coefficients (ρ) and p-values corrected for multiple testing using the false discovery rate (FDR) method. MMSE: Mini Mental State Examination corrected for age and education level.

	MMSE	
Acylcarnitine	**ρ**	**p[a]**
C14:1	0.53	0.009
C12:1	0.51	0.009
C18:1	0.51	0.009
C16	0.49	0.012
C14:2	0.48	0.012
C12	0.46	0.014
C8	0.46	0.014
C10	0.41	0.030
C2	0.39	0.038

[a] FDR corrected.

Table 3. Correlations between regional grey matter volumes and plasma levels of decanoylcarnitine (C10) occurring in the study groups. No significant correlations between grey matter volumes and ACC plasma levels were found in HC subjects.

Grey matter labels for cluster peak (BA[a])	Correlation coefficient	Cluster extent (mm^3)	p[b]	t-value[c]	equivZ[d]	x,y,z (mm)[e]
Group: MCI						
Left precentral gyrus (BA 3-4-6)	0.74	695	0.028	5.79	4.60	-20, -16, 61
Group: AD						
Right precentral gyrus (BA 3-4-6)	0.69	168	0.032	4.33	3.57	30, -25. 46

[a] Brodman area; [b] Family-Wise Error corrected; [c] Voxelwise t-value; [d] Voxelwise z-score; [e] Montreal Neurological Institute (MNI) coordinates.

Supplementary Table 1. Cognitive and neuropsychological battery administered to healthy control (HC) subjects, mild cognitive impairment (MCI) and Alzheimer's disease (AD) patients. The table depicts mean scores with the corresponding standard deviations (SD) as well as p values from Levene test for homogeneity of variance, ANOVA or Kruskal-Wallis test, and Fischer LSD test or multiple comparison of mean ranks. Cut-off values are also shown. Scores are corrected for age and education levels. NA: not applicable. NS: not significant.

				Mean (SD)					Fisher LSD post-hoc test/multiple comparison of mean ranks, p		
Cognitive Measures	**Dependent Measure (Range)**	**Domain Assessed**	**cut-off**	**HC**	**MCI**	**AD**	**Levene test, p**	**ANOVA/Kruskal-Wallis, p**	**HC vs MCI**	**HC vs AD**	**MCI vs AD**
Benton Face Recognition	0-54	Face recognition	38	47 (4)	46 (5)	28 (19)	<0.001	0.006	NS	0.005	0.023
MDB Rey's 15-word Immediate Recall [RIR]	0-75	Memory	29	45 (8)	29 (7)	20 (10)	NS	<0.001	<0.001	<0.001	<0.001
MDB Rey's 15-word Delayed Recall [RDR]	0-15	Memory	5	10 (3)	5 (3)	2 (3)	NS	<0.001	<0.001	<0.001	<0.001
Raven's Progressive Matrices' 47 [PM47]	0-36	Deductive reasoning	24	29 (6)	27 (4)	17 (7)	NS	<0.001	NS	<0.001	<0.001
Immediate Visual Memory	0-22	Memory	14	21 (1)	20 82)	14 (5)	<0.001	<0.001	NS	<0.001	<0.001
Copy of Rey-Osterrieth's complex picture test (CROP)	0-36	Praxis	24	32 (3)	29 (6)	21 (9)	0.005	<0.001	0.005	<0.001	0.031
Recall of Rey-Osterrieth's complex picture test (ROP)	0-36	Memory/Praxis	6	17 (5)	11 (4)	5 (5)	NS	<0.001	<0.001	<0.001	0.011
Phonological Verbal Fluency	-	Language	17	33 810)	30 (9)	22 (10)	NS	0.003	NS	<0.001	<0.001
Semantic Verbal Fluency (SVF)	-	Language	12	19 (5)	15 (3)	9 (5)	<0.001	<0.001	NS	<0.001	0.002
Freehand Copying of Drawings	0-12	Praxis	7	11 (1)	10 (2)	7 (3)	0.002	<0.001	NS	<0.001	<0.001
Copying of drawings with programming	0-70	Praxis	62	65 (5)	64 (5)	48 (17)	<0.001	<0.001	NS	<0.001	<0.001
Sentence Construction	0-25	Language	8.72	21 (6)	16 (9)	10 (9)	0.014	<0.001	NS	<0.001	NS
Multiple Features Targets Cancellation Task (MFTC) time of performance (sec)	-	Attention	165	60 (20)	89 (47)	141 (112)	<0.001	<0.001	<0.001	<0.001	NS
Multiple Features Targets Cancellation Task (MFTC) hits	0-13		9.9	11 (2)	10 (2)	9 (5)	0.009	0.03	0.037	NS	NS
Multiple Features Targets Cancellation Task (MFTC) false alarms	0-67		2.2	0.2 (0.5)	1 (1)	5 (7)	<0.001	<0.001	NS	0.003	NS
Modified Wisconsin Card Sorting Test (MWCST) number of categories	0-6	Executive functions	3	5.7 (0.8)	5 (2)	3 (2)	<0.001	<0.001	NS	0.007	NS
Modified Wisconsin Card Sorting Test (MWCST) perseverative errors	0-47		6.4	2 (3)	3 (2)	7 (5)	NS	0.009	NS	0.002	0.014
Modified Wisconsin Card Sorting Test (MWCST) non perseverative errors	0-48		NA	2 (2)	4 (4)	5 (3)	0.004	0.005	0.026	0.036	NS

Supplementary Table 2. Electrospray ionization mass spectrometry (ESI-MS) acquisition parameters employed for the analysis of plasma acylcarnitines (ACCs). MS/MS transitions for each analysed ACC and the corresponding internal standard (IS, shown in bold), the optimal cone potential (V), and collision energy (eV) are shown for each analyte. The capillary potential was 3.5kV.

Abbreviation IS	Full name	Transition	Cone potential	Collision energy
C0 **D9C0**	Carnitine	161.9>102.9 170.9>102.9	60	14
C2 **D3C2**	Acetylcarnitine	204.0>84.9 207.0>84.9	60	14
C3 **D3C3**	Propionylcarnitine	218.0>84.9 221.0>84.9	60	15
C4 C3DC/C4OH **D3C4**	Butyrylcarnitine Malonylcarnitine/3-Hydroxy-butyrylcarnitine	232.0>84.9 248.0>84.9 235.0>84.9	60	15
C5 C5:1 C4DC/C5OH **D9C5**	Valerylcarnitine Tiglylcarnitine Methylmalonylcarnitine/3-Hydroxy-valerylcarnitine	246.0>84.9 244.0>84.9 262.0>84.9 255.0>84.9	70	16
C5DC/C6OH C6DC **D6C5DC**	Glutarylcarnitine/3-Hydroxy-hexanoylcarnitine Adipylcarnitine	276.0>84.9 290.0>84.9 282.0>84.9	70	20
C6 **D3C6**	Hexanoylcarnitine	260.1>84.9 263.1>84.9	65	16
C8:1 C8 **D3C8**	Octenoylcarnitine Octanoylcarnitine	286.1>84.9 288.1>84.9 291.1>84.9	75	18

Supplementary Table 2. Continued.

Abbreviation IS	Full name	Transition	Cone potential	Collision energy
C10	Decanoylcarnitine	316.1>84.9	75	19
C10:2	Decadienoylcarnitine	312.1>84.9		
C10:1	Decenoylcarnitine	314.1>84.9		
D3C10		319.1>84.9		
C12:1	Dodecenoylcarnitine	342.1>84.9	75	20
C12	Dodecanoylcarnitine	344.1>84.9		
D3C12		347.1>84.9		
C14	Tetradecanoylcarnitine (myristoylcarnitine)	372.2>84.9	75	21
C14:1	Tetradecenoylcarnitine	370.2>84.9		
C14:2	Tetradecadienoylcarnitine	368.2>84.9		
C14:OH	3-Hydroxy-tetradecanoylcarnitine	388.2>84.9		
D3C14		375.2>84.9		
C16:1	Hexadecenoylcarnitine	398.2>84.9	75	23
C16	Hexadecanoylcarnitine (palmitoylcarnitine)	400.2>84.9		
C16:1-OH	3-Hydroxy-hexadecenoylcarnitine	414.2>84.9		
C16-OH	3-Hydroxy-hexadecanoylcarnitine	416.2>84.9		
D3C16		403.2>84.9		
C18	Octadecanoylcarnitine (Stearoylcarnitine)	428.3>84.9	80	24
C18:1	Octadecenoylcarnitine (Oleylcarnitine)	426.3>84.9		
C18:2	Octadecadienoylcarnitine (Linoleylcarnitine)	424.3>84.9		
C18:1-OH	3-Hydroxy-octadecenoylcarnitine	442.3>84.9		
C18-OH	3-Hydroxy-octadecanoylcarnitine	444.3>84.9		
D3C18		431.3>84.9		

Supplementary Table 3. Plasma acylcarnitine profiling of HC, MCI and AD participants. Data are expressed in µmol L^{-1}. p-values less than 0.050 are shown in bold. NS: not significant.

	HC		MCI		AD						
Acylcarnitine	**Mean (SD[a])**	**Median (Interquartile range)**	**Mean (SD[a])**	**Median (Interquartile range)**	**Mean (SD[a])**	**Median (Interquartile range)**	**Levene test, p**	**ANOVA/Kruskal-Wallis test, F[b]/H[c] (p)[d]**	**HC vs MCI[e]**	**HC vs AD[e]**	**MCI vs AD[e]**
C0	34 (7)	33 (9)	37 (8)	36 (9)	32 (7)	34 (9)	0.61	3.55 (**0.032**)	NS	NS	**0.009**
C2	9 (3)	10 (5)	9 (2)	9 (3)	8 (4)	7 (2)	0.28	4.62 **(0.012)**	NS	**0.009**	**0.010**
C3	0.5 (0.2)	0.5 (0.1)	0.4 (0.2)	0.4 (0.2)	0.5 (0.2)	0.4 (0.3)	0.38	1.53 (0.22)	NS	NS	NS
C4	0.2 (0.1)	0.23 (0.06)	0.3 (0.2)	0.2 (0.1)	0.2 (0.1)	0.2 (0.1)	0.083	0.51 (0.60)	NS	NS	NS
C5	0.13 (0.04)	0.12 (0.04)	0.13 (0.04)	0.11 (0.05)	0.13 (0.06)	0.12 (0.09)	0.26	0.056 (0.95)	NS	NS	NS
C5DC[f]/C6OH	0.12 (0.03)	0.11 (0.04)	0.11 (0.03)	0.11 (0.03)	0.10 (0.03)	0.10 (0.03)	0.99	1.58 (0.21)	NS	NS	NS
C8:1	0.05 (0.02)	0.04 (0.03)	0.05 (0.06)	0.04 (0.02)	0.04 (0.02)	0.04 (0.01)	0.40	1.36 (0.26)	NS	NS	NS
C8	0.2 (0.1)	0.2 (0.1)	0.2 (0.2)	0.2 (0.1)	0.12 (0.06)	0.11 (0.09)	**0.004**	17.54 **(<0.001)**	NS	**0.001**	**<0.001**
C6DC[f]	0.18 (0.7)	0.15 (0.08)	0.16 (0.07)	0.14 (0.08)	0.16 (0.09)	0.14 (0.07)	0.93	0.56 (0.57)	NS	NS	NS
C10:1	0.11 (0.04)	0.11 (0.05)	0.13 (0.06)	0.11 (0.09)	0.08 (0.03)	0.08 (0.03)	**<0.001**	18.46 **(<0.001)**	NS	**0.003**	**<0.001**
C10	0.3 (0.1)	0.3 (0.2)	0.4 (0.2)	0.3 (0.3)	0.2 (0.1)	0.2 (0.1)	**0.004**	19.50 **(<0.001)**	NS	**<0.001**	**<0.001**
C12:1	0.09 (0.03)	0.09 (0.05)	0.10 (0.09)	0.09 (0.06)	0.06 (0.03)	0.06 (0.04)	**0.043**	19.68 **(<0.001)**	NS	**0.001**	**<0.001**
C12	0.07 (0.03)	0.08 (0.04)	0.09 (0.04)	0.08 (0.05)	0.05 (0.02)	0.05 (0.03)	**0.025**	16.37 **(<0.001)**	NS	**0.003**	**<0.001**
C14:2	0.03 (0.01)	0.03 (0.01)	0.03 (0.02)	0.03 (0.02)	0.02 (0.01)	0.02 (0.02)	**0.007**	19.56 **(<0.001)**	NS	**0.002**	**<0.001**
C14:1	0.10 (0.04)	0.10 (0.05)	0.12 (0.05)	0.11 (0.06)	0.07 (0.04)	0.07 (0.04)	0.23	10. 43 **(<0.001)**	NS	**0.009**	**<0.001**

[a] Standard deviation; [b] degrees of freedom: 2, 117; [c] degrees of freedom: 2, 120; [d] FDR corrected; [e] Fischer LSD post-hoc test or multiple comparison of mean ranks. [f] DC: dicarboxy-acylcarnitine.

Supplementary Table 3. Continued.

	HC		MCI		AD						
Acylcarnitine	Mean (SD[a])	Median (Interquartile range)	Mean (SD[a])	Median (Interquartile range)	Mean (SD[a])	Median (Interquartile range)	Levene test, p	ANOVA/Kruskal-Wallis test, F[b]/H[c] (p)[d]	HC vs MCI[e]	HC vs AD[e]	MCI vs AD[e]
C14	0.030 (0.008)	0.030 (0.005)	0.03 (0.01)	0.03 (0.02)	0.03 (0.01)	0.03 (0.01)	**0.009**	3.09 (0.21)	NS	NS	NS
C16	0.11 (0.02)	0.10 (0.02)	0.11 (0.03)	0.11 (0.04)	0.10 (0.03)	0.10 (0.04)	**0.042**	2.93 (0.23)	NS	NS	NS
C18:2	0.038 (0.009)	0.04 (0.02)	0.05 (0.01)	0.04 (0.02)	0.04 (0.01)	0.03 (0.02)	**0.026**	6.90 (**0.032**)	NS	NS	NS
C18:1	0.16 (0.04)	0.15 (0.05)	0.17 (0.04)	0.16 (0.07)	0.14 (0.05)	0.14 (0.06)	0.18	3.54 (**0.033**)	NS	NS	**0.009**
C18	0.042 (0.009)	0.04 (0.01)	0.04 (0.01)	0.04 (0.02)	0.04 (0.01)	0.04 (0.02)	0.093	0.56 (0.57)	NS	NS	NS

[a] Standard deviation; [b] degrees of freedom: 2, 117; [c] degrees of freedom: 2, 120; [d] FDR corrected; [e] Fischer LSD post-hoc test or multiple comparison of mean ranks; [f] DC: dicarboxy-acylcarnitine.

Supplementary Table 4. Significant correlations between plasma levels of beta-hydroxybutyric acid (b-HBA) and plasma acylcarnitines in AD patients. Data are Spearman's correlation coefficients (ρ) and p-values corrected for multiple testing using the false discovery rate (FDR) method.

	b-HBA	
Acylcarnitine	**ρ**	**p[a]**
C2	0.79	<0.001
C14	0.75	<0.001
C14:2	0.69	0.004
C14:1	0.66	0.007
C12	0.64	0.008
C12:1	0.62	0.010
C10	0.54	0.038

[a] FDR corrected.

Supplementary Table 5. Correlations between regional grey matter volumes and plasma levels of octanoylcarnitine (C8) occurring in the study groups. No significant correlations between grey matter volumes and ACC plasma levels were found in HC subjects.

Grey matter labels for cluster peak (BA[a])	Correlation coefficient	Cluster extent (mm^3)	p[b]	t-value[c]	equivZ[d]	x,y,z (mm)[e]
Group: MCI						
Left precentral gyrus (BA 3-4-6)	0.71	429	0.033	5.82	4.56	-20, -16, 66
Group: AD						
Right precentral gyrus (BA 3-4-6)	0.63	123	0.038	4.17	3.52	28, -23, 49

[a] Brodman area; [b] Family-Wise Error corrected; [c] Voxelwise t-value; [d] Voxelwise z-score; [e] Montreal Neurological Institute (MNI) coordinates.

Supplementary Table 6. Correlations between regional grey matter volumes and plasma levels of dodecanoylcarnitine (C12) occurring in the study groups. No significant correlations between grey matter volumes and ACC plasma levels were found in HC subjects.

Grey matter labels for cluster peak (BA[a])	Correlation coefficient	Cluster extent (mm^3)	p[b]	t-value[c]	equivZ[d]	x,y,z (mm)[e]
Group: MCI						
Left precentral gyrus (BA 3-4-6)	0.66	98	0.040	5.70	4.38	-22, -18, 62
Group: AD						
Right precentral gyrus (BA 3-4-6)	0.67	63	0.042	4.03	3.48	29, -19, 54

[a] Brodman area; [b] Family-Wise Error corrected; [c] Voxelwise t-value; [d] Voxelwise z-score; [e] Montreal Neurological Institute (MNI) coordinates.

Figure legends

Figure 1. Acylcarnitine profiling of plasma collected from healthy HC, MCI and AD individuals. Scatter plots show mean plasma concentrations of free carnitine (C0), acetylcarnitine (C2), octanoylcarnitine (C8), decenoylcarnitine (C10:1), decanoylcarnitine (C10), dodecenoylcarnitine (C12:1), dodecanoylcarnitine (C12), tetradecadienoylcarnitine (C14:2), tetradecenoylcarnitine (C14:1), and octadecenoylcarnitine (C18:1) assayed in the study participants. Green squares indicate HC subjects. Blue and red squares indicate MCI or AD patients, respectively. Red lines and the plus symbols indicate median and mean values, respectively. Data are expressed in μmol L^{-1}. * indicates p-values less than 0.050 (one-way ANOVA followed by Fisher LSD test or Kruskal-Wallis test followed by multiple comparisons of mean ranks).

Figure 2. Correlation heat maps and hierarchical clustering for plasma acylcarnitines of HC, MCI or AD subjects. Heat maps show correlation coefficients calculated by Spearman's rank correlation analysis of plasma ACCs in HC subjects (**A**), MCI (**B**), and AD patients (**C**). Maps are expressed in pseudocolors ranging from red (positive correlation) to green (negative correlation). Hierarchical cluster analysis of target metabolites was performed taking in account correlation coefficients set to cluster ACCs that showed similar trends in the three study cohorts. Note that medium-chain ACCs are clustered with high degree of positive correlation in each study group (white boxes).

Figure 3. Multivariate data and ROC analysis of plasma acylcarnitine profiles of HC, MCI and AD subjects. Heatmap visualization of hierarchiacal clustering analysis based on plasma ACC profiles of the three study groups **(A).** Euclidean distance was used for clustering. Each bar represents an ACC coded with pseudocolors in accordance with metabolite concentrations and expressed with a normalized scale ranging from blue (low level) to red (high level). Rows indicate samples while columns depict analysed ACCs. PLS-DA score plot based on plasma ACC concentrations found in the three study groups **(B)**. Variable importance on projection (VIP) plot (**C**). VIP scores higher than 1 indicate a high relevance for the selected ACC in the predictive model. Receiver operating characteristic (ROC) analysis discriminating HC from MCI subjects **(D)**, HC from AD subjects **(E)**, and MCI from AD subjects **(F)**. Values of the area under the curve (AUC) with confidence intervals (95% confidence level) are shown along with optimal cut-off corresponding to the higher

specificity and sensitivity for each potential biomarker. Ratios between medium-chain ACCs (C14:1/ C14 and C12:1/ C14) were the best predictors in the discrimination of AD from HC or MCI subjects.

Figure 4. Relationship between grey matter (GM) volumes and plasma levels of decanoylcarnitine (C10) occurring in MCI and AD patients. Upper panels (**A and B**) depict representative axial slices of the Montreal Neurological Institute (MNI) template showing two clusters in which positive variations of GM volumes correlate with higher plasma levels of C10. Panel A depicts a cluster located in the left precentral gyrus of MCI patients. Panel B depicts a cluster in the right precentral gyrus of AD patients. Lower panels (**C and D**) show scatter graphs depicting correlations between GM volumes and plasma levels of C10 in the cortical areas illustrated in A for MCI and B for AD patients. Green circles indicate individual values for MCI, blue circles indicate individual values for AD. Red plots refer to values found in HC subjects and are shown as reference points for comparison with MCI or AD values. Scatter plots are created by plotting mean volumetric values of areas in which correlations are statistically significant. Coordinates (Z values) are in Montreal Neurological Institute (MNI) space. Linear fits are shown in dotted lines.

Figure 5. Plasma 2-hydroxybutyric acid (b-HBA) concentrations in HC, MCI, and AD patients. Scatter plots show mean concentrations of b-HBA measured in plasma collected from the study participants. Green squares indicate HC subjects. Blue and red squares indicate MCI or AD patients, respectively. Red lines and the plus symbols indicate median and mean values, respectively. Data are expressed inμmol L^{-1}. * indicates p-values less than 0.050 (one-way ANOVA followed by Fisher LSD test).

Figure 6. Correlations between plasma 2-hydroxybutyric acid (b-HBA), plasma acylcarnitines (ACCs) and Mini Mental State Examination (MMSE) scores in HC, MCI, and AD subjects. The upper panels show bar graphs depicting correlation coefficients of ACCs and b-HBA plasma concentrations in HC (**A**), MCI subjects (**B**), and AD patients (**C**). Values are ranging from -1 (negative correlation) to 1 (positive correlation) and calculated by Spearman's correlation analysis. Red and green bars indicate positive or negative correlations, respectively. Plasma ACCs marked with * are significantly associated with plasma b-HBA levels ($p<0.050$). Note that no significant

correlations are found in HC and MCI subjects while medium-chain ACCs positively correlate with b-HBA in AD patients. The lower panels show correlation plots depicting the association between plasma b-HBA levels and MMSE scores found in HC (**D**), MCI subjects (**E**), and AD patients (**F**). No significant correlations are found in HC and MCI subjects while significant association between b-HBA and MMSE is found in AD patients. MMSE scores are corrected for age and education level.

Supplementary Figure 1. Correlations between levels of medium-chain plasma acylcarnitines (ACCs) and Mini Mental State Examination (MMSE) scores occurring in AD patients. Panels show correlation plots depicting significant associations between plasma levels of acetylcarnitine (C2), octanoylcarnitine (C8), decanoylcarnitine (C10), dodecenoylcarnitine (C12:1), dodecanoylcarnitine (C12), tetradecadienoylcarnitine (C14:2), tetradecenoylcarnitine (C14:1), palmitoylcarnitine (C16), oroctadecenoylcarnitine (C18:1) and MMSE scores of AD patients. Correlation significance was assessed by Spearman's correlation analysis. FDR corrected p-values less than 0.050 were considered statistically significant.

Supplementary Figure 2. Relationship between grey matter (GM) volumes and plasma levels of octanoylcarnitine (C8) occurring in MCI and AD patients. Upper panels (**A and B**) depict representative axial slices of the Montreal Neurological Institute (MNI) template showing two clusters in which positive variations of GM volumes correlate with higher plasma levels of C8. Panel A depicts a cluster located in the left precentral gyrus of MCI patients. Panel B depicts a cluster in the right precentral gyrus of AD patients. Lower panels (**C and D**) show scatter graphs depicting correlations between GM volumes and plasma levels of C8 in the cortical areas illustrated in A for MCI and B for AD patients. Green circles indicate individual values for MCI, blue circles indicate individual values for AD. Red plots refer to values found in HC subjects and are shown as reference points for comparison with MCI or AD values. Scatter plots are created by plotting mean volumetric values of areas in which correlations are statistically significant. Coordinates (Z values) are in Montreal Neurological Institute (MNI) space. Linear fits are shown in dotted lines.

Supplementary Figure 3. Relationship between grey matter (GM) volumes and plasma levels of dodecanoylcarnitine (C12) occurring in MCI and AD patients. Upper panels (**A and B**) depict representative axial slices of the Montreal Neurological Institute (MNI) template showing two

clusters in which positive variations of GM volumes correlate with higher plasma levels of C12. Panel A depicts a cluster located in the left precentral gyrus of MCI patients. Panel B depicts a cluster in the right precentral gyrus of AD patients. Lower panels (**C and D**) show scatter graphs depicting correlations between GM volumes and plasma levels of C12 in the cortical areas illustrated in A for MCI and B for AD patients. Green circles indicate individual values for MCI, blue circles indicate individual values for AD. Red plots refer to values found in HC subjects and are shown as reference points for comparison with MCI or AD values. Scatter plots are created by plotting mean volumetric values of areas in which correlations are statistically significant. Coordinates (Z values) are in Montreal Neurological Institute (MNI) space. Linear fits are shown in dotted lines.

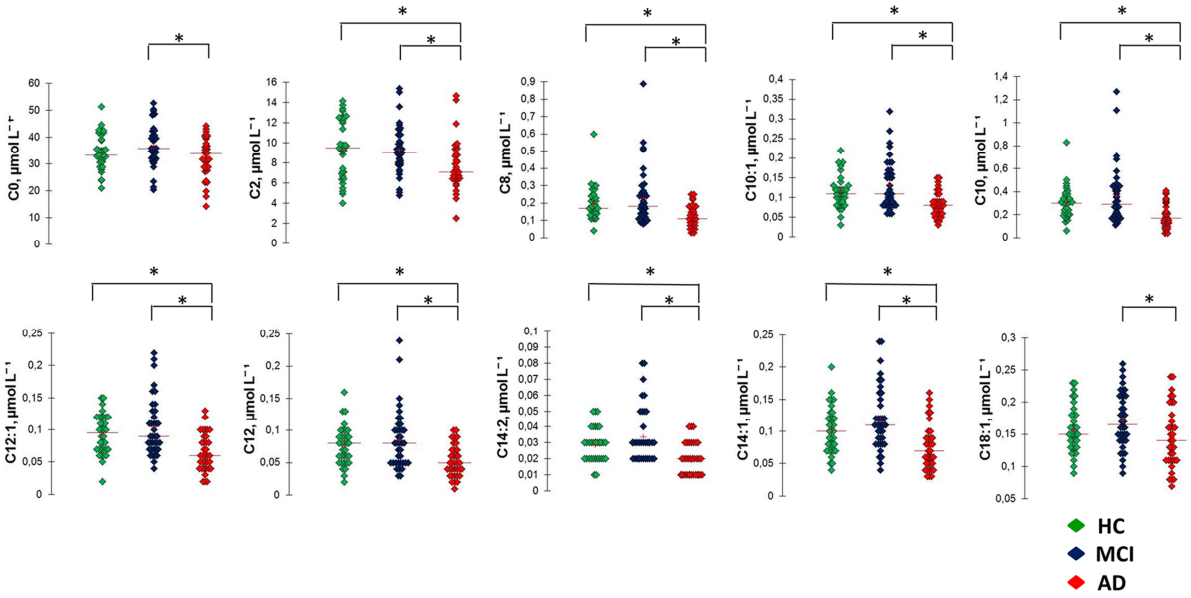

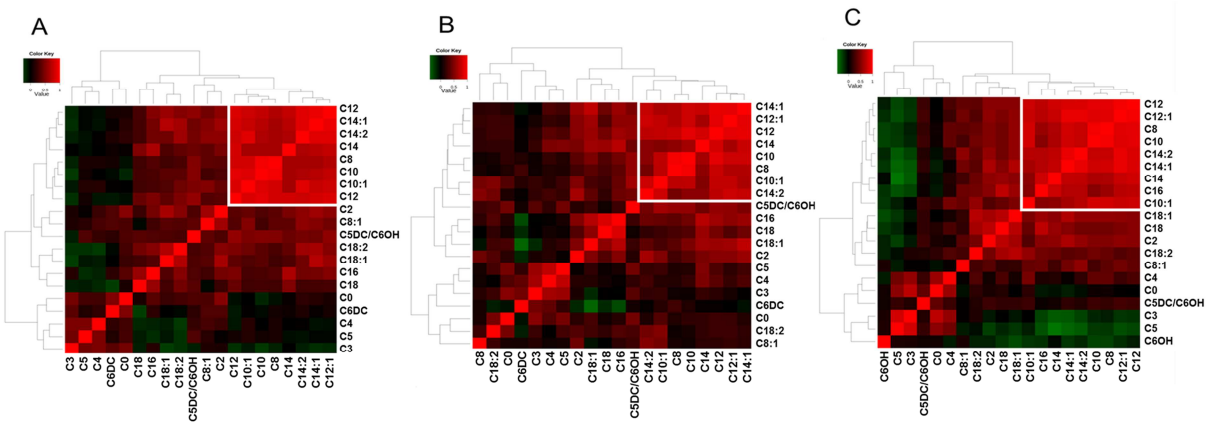

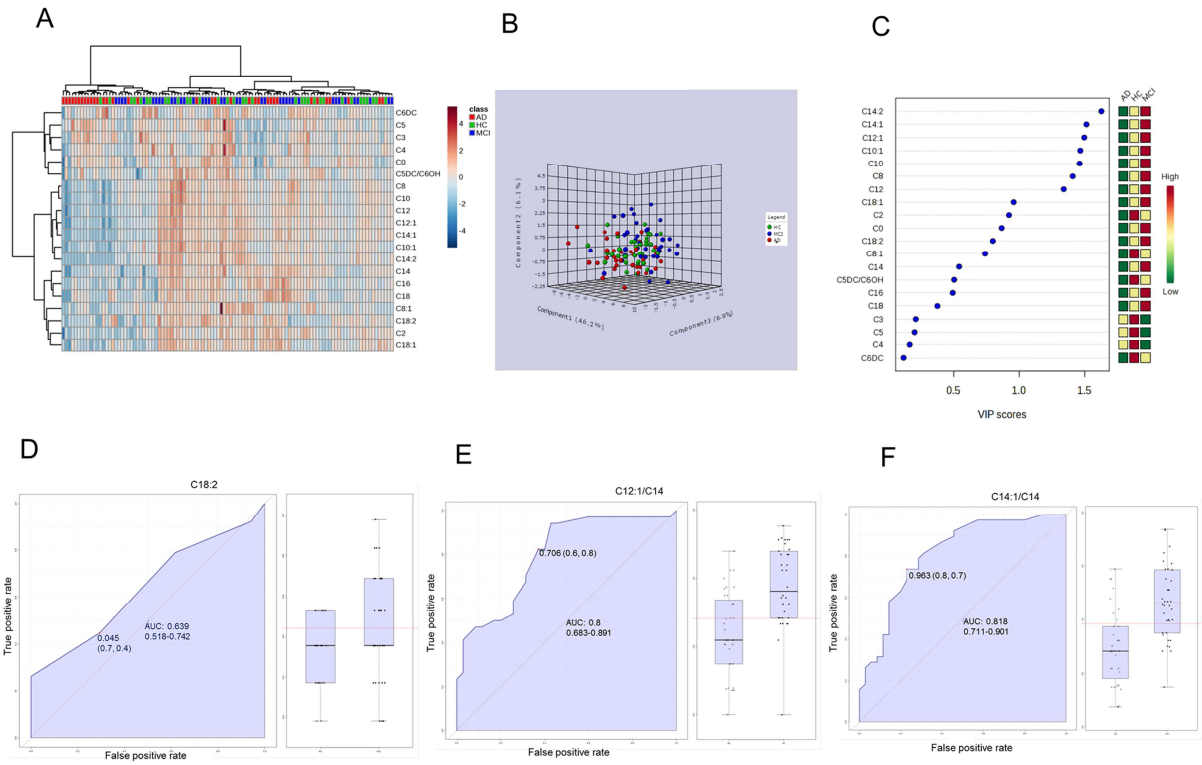

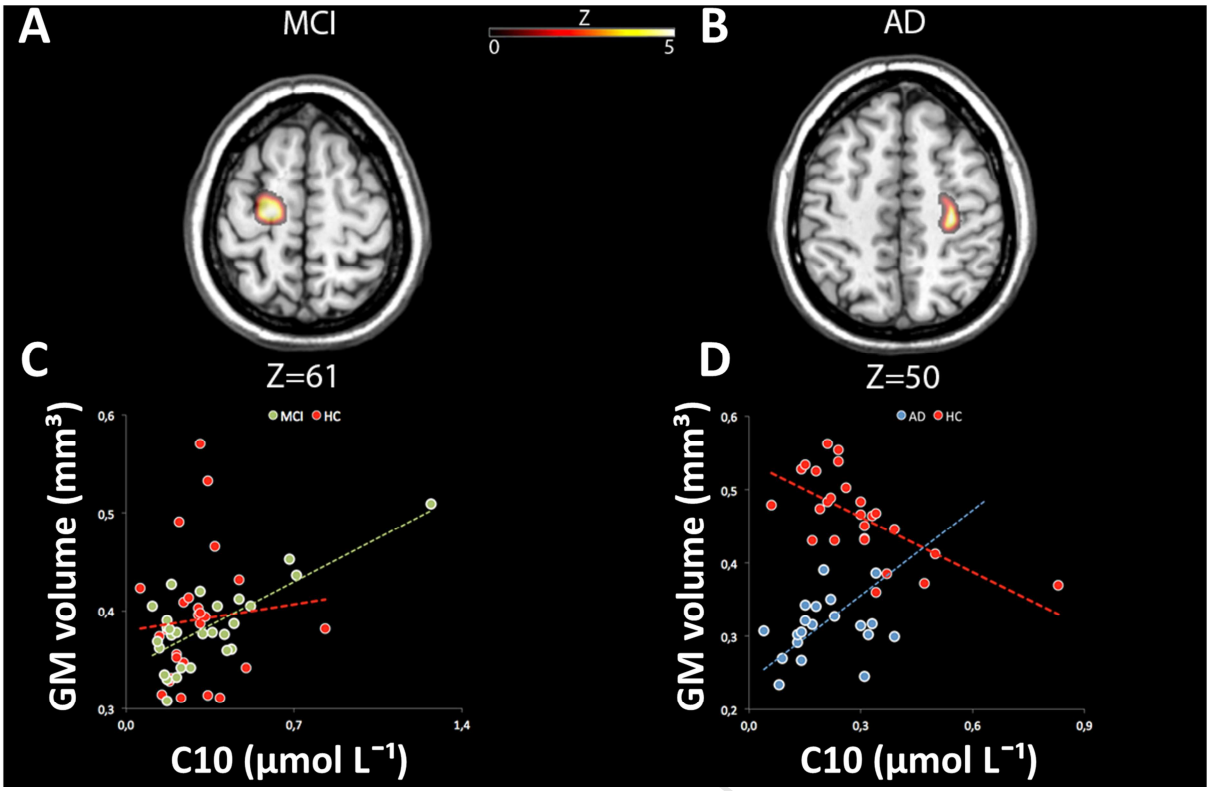

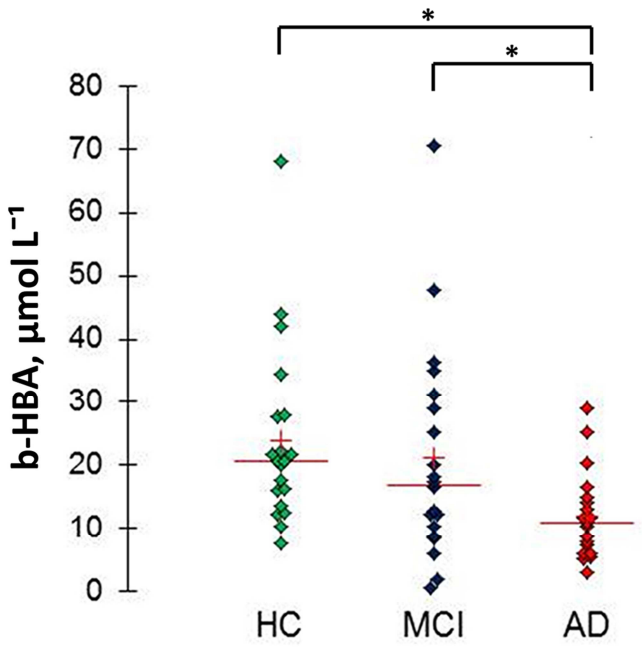

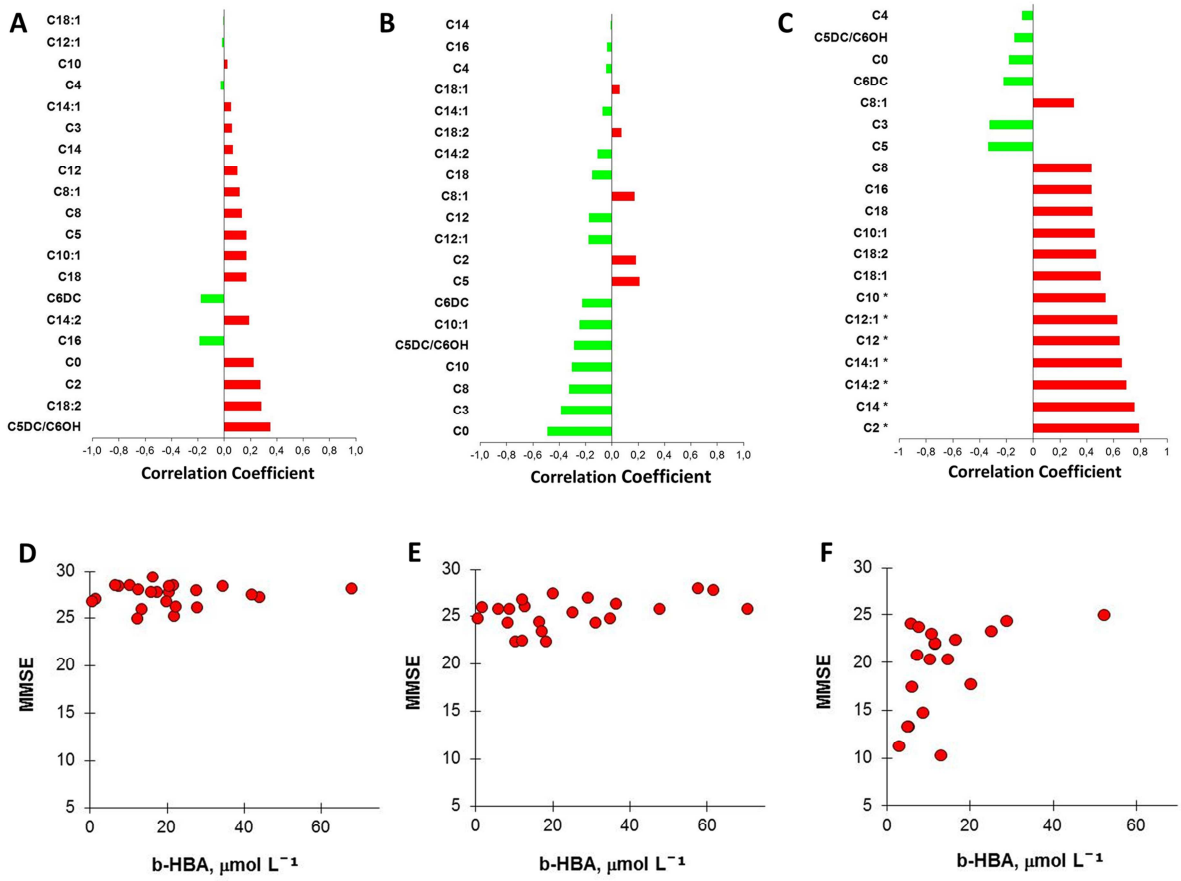

Highlights

Medium-chain plasma acylcarnitines decrease in Alzheimer's disease patients.

Low ACCs are associated to lower prefrontal regional GM volumes and cognitive impairment in AD.

Alteration of ACC metabolism may be associated with impaired ketogenesis in AD.